Accepted Manuscript

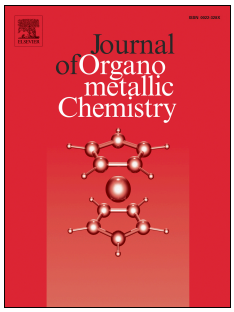

Fluxional Pd(II) NHC complexes – Synthesis, structure elucidation and catalytic studies

Miroslav Dangalov, Malinka Stoyanova, Petar Petrov, Martin Putala, Nikolay G. Vassilev

PII: S0022-328X(16)30177-2

DOI: 10.1016/j.jorganchem.2016.05.002

Reference: JOM 19491

To appear in: *Journal of Organometallic Chemistry*

Received Date: 5 February 2016

Revised Date: 14 April 2016

Accepted Date: 2 May 2016

Please cite this article as: M. Dangalov, M. Stoyanova, P. Petrov, M. Putala, N.G. Vassilev, Fluxional Pd(II) NHC complexes – Synthesis, structure elucidation and catalytic studies, *Journal of Organometallic Chemistry* (2016), doi: 10.1016/j.jorganchem.2016.05.002.

Who is who? (combined DNMR and DFT approach)

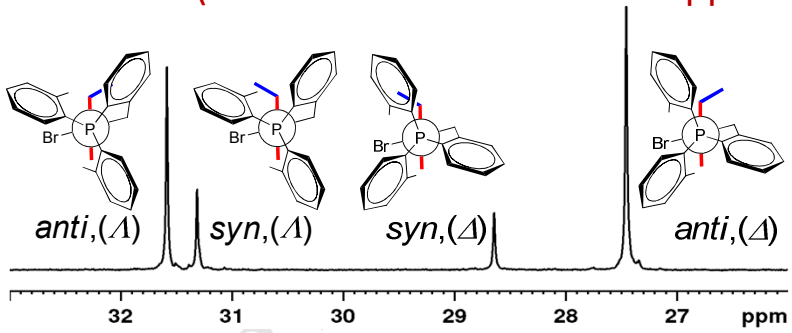

Fluxional Pd(II) NHC Complexes - Synthesis, Structure Elucidation and Catalytic Studies

Miroslav Dangalov [a], Malinka Stoyanova [a], Petar Petrov [b], Martin Putala [c] and Nikolay G. Vassilev [a,*]

[a] *Institute of Organic Chemistry with Center of Phytochemistry, 9, Acad. G. Bonchev Str., 1113 Sofia, Bulgaria*
[b] *Department of Organic Chemistry, Faculty of Chemistry and Pharmacy, Sofia University St. Kliment Ohridsky, 1, James Bourchier Blvd., 1164 Sofia, Bulgaria*
[c] *Department of Organic Chemistry, Faculty of Natural Sciences, Comenius University in Bratislava, Mlynska dolina, Ilkovičova 6, 84215 Bratislava, Slovakia*

ABSTRACT: Four catalytically relevant Pd(II) complexes involving N-heterocyclic carbenes (NHCs) and bidentate N- and P-donor ligands were synthesized and characterized. The structures and conformations of the complexes were elucidated on the basis of combination of dynamic NMR and DFT studies. Conformational studies in respect to hindered rotation around C-N_{donor} and Pd-C_{NHC} bonds were performed resulting in surprisingly good agreement between the calculated and the experimental results. The results from dynamic NMR and DFT studies confirm hindered rotation around the C-N bond in 1,3-disubstituted imidazole complexes. The fluxional behavior of P-donor ligands includes exchange between left-handed and right-handed phosphine propellers. The catalytic studies of 1,3-disubstituted 4,5-fused imidazole complexes produced excellent activities in Suzuki–Miyaura Reaction.

Keywords: Palladium(II), NHC complexes, dynamic NMR, DFT calculations, catalytic studies

1. Introduction

N-Heterocyclic carbenes (NHC) are state of the art ligands in organometallic chemistry [1-6] and catalysis [7-10]. The nitrogen atoms in the heterocycle offer possibilities for tuning the ligand structure - through changes in the N substituents, the steric demands and electronic properties of the ligand can be modified to provide complexes with enhanced catalytic performances [11-14]. Also, various functional groups can be introduced, resulting in complexes with wider applications [15, 16]. The introduction of a suitable donor group can lead to versatile structures in ditopic complexes or enhanced catalytic performance of complexes with hemilabile ligands [17-22]. Potentially antibacterial compounds have also been synthesized by the introduction of a biologically active function [23-25]. In addition, complexes of bifunctional ligands can be immobilized or their solubilities altered by suitable functionalization to afford recoverable catalysts [26-30].

During the last decade, numerous applications of N-heterocyclic carbenes (NHCs) as ligands in all areas of transition metal catalysis have been found [7, 31-33]. NHCs are strong, neutral *σ*-donor ligands which form very stable bonds with the majority of transition metals [7, 33]. NHC complexes also possess greater thermal stability than their phosphane analogues, which benefits the catalyst stability. The most successful NHC cores are derived from imidazolium and 4,5-dihydroimidazolium salts, that have bulky substituents at both nitrogen atoms [31, 34]. The steric and electronic properties NHCs can be tuned independently, because the *N*-substituents, are not directly connected to the carbene carbon atom and their influence on the electronic density of this atom is small [35, 36]. The heterocyclic core determines the electronic properties of the carbene [37] and fusing an additional aromatic ring provides further possibilities for fine tuning of the electronic properties of the NHCs [38].

* Corresponding author. Tel.: +359 2 9606172; fax: +359 2 8700225
E-mail: niki@orgchm.bas.bg (N. G. Vassilev)

Recently 4-amino-3-nitro substituted 1,8-naphthalimides as potential photoactive sensors and starting compounds for further transformations to fluorescent sensors have been reported [39]. The application of 1,8-naphthalimide derivatives as the photoactive units for design of optical chemosensors for metal cations and protons with different mechanisms of analyte binding signal transduction and different receptors was recently reviewed [40]. In an ongoing investigation on catalysis we synthesized carbene complexes based on the fluorescent naphthalimide core connected/fused to an imidazolium salt. Since the fluxional behavior of a molecule may have a dramatic impact on the relaxation pathways from its respective excited states, it was important to study the dynamics of these newly synthesized compounds in details. In this study we introduce the 1,8-naphthalimides as an *N* substituent and as a fused aromatics to the NHC to form catalytically relevant Pd(II) complexes with additional bidentate *N*- and *P*-donor ligands to the metal.

Herein, we report the synthesis of novel Pd N-heterocyclic carbene complexes. Two of them, **1** and **2**, (Fig. 1) are 1,3-disubstituted imidazole NHC complexes (*1,3-disubstituted*), while the others two are the corresponding 1,3-disubstituted 4,5-fused imidazole NHC complexes (*4,5-fused*), **3** and **4**. Conformational exchanges occurred in solution at rates that were intermediate on the NMR time scale. The ^{1}H NMR signals of complexes **1, 2** and **4** were broad at room temperature and therefore, it was necessary to study their NMR spectra at lower temperatures. The NMR spectra of complex **3** were recorded at room temperature due to the presence of the single preferred conformer. The possible conformers, exchange routes and the origin of the observed exchanged were studied by combination of dynamic NMR and DFT calculations.

The assignment of VT NMR spectra of studied complexes is a challenging task that required combination of dynamic NMR study and DFT calculation. Dynamic NMR study using 2D EXSY spectra provides information about the exchange routes and the corresponding rate constants can be calculated directly from the volume integrals. The DFT calculations of GS structures provide information about thermodynamic stability of possible conformers. Calculating the theoretical populations and comparing them with the experimental one allows the conformers assignment. If given NMR chemical shifts are sensitive to the exchange, comparison of DFT calculated and the experimental values can confirm the assignment of conformers. The comparison of experimental and DFT calculated barriers can reveal the exchange mechanism. This integrated approach, which combines methods of dynamic NMR spectroscopy and computational chemistry was successfully applied recently for studying the structure and exchange mechanism of *ortho*-diphenylphosphinobenzenecarboxamide ligands[41] and atropisomers of 2,2′-diaryl-1,1′-binaphthalenes containing three stereogenic axes[42].

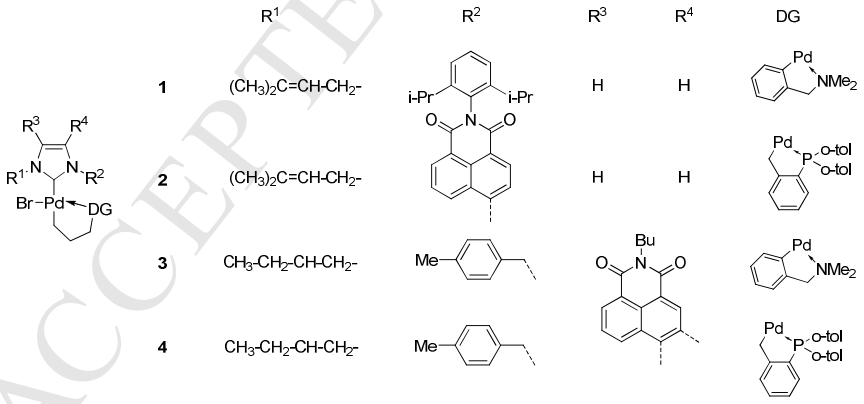

Figure 1. Complexes **1-4** (o-tol = *ortho*-tolyl)

2. Results and Discussion

Synthesis of complexes

The first step of synthesis of the desired *1,3-disubstituted* Pd(II) NHC complexes **1** and **2** was preparation of imidazolium salt **NHC.HBr**, which was synthesized from commercial 4-bromo-1,8-naphthalic anhydride (Scheme 1). 6-Bromo substituted naphthalimide **II** was prepared by reaction of 2,6-diisopropylaniline and 4-bromo-1,8-naphthalic anhydride in refluxing acetic acid according the literature [43]. The naphthalimide **II** reacts with imidazole in the

presence of CuI, proline-based ligand and Cs_2CO_3 in DMF to obtain compound **III** [44], which was quaternized with 3,3-dimethylallyl bromide in ethyl acetate to yield the corresponding imidazolium bromide salt (**NHC.HBr**).

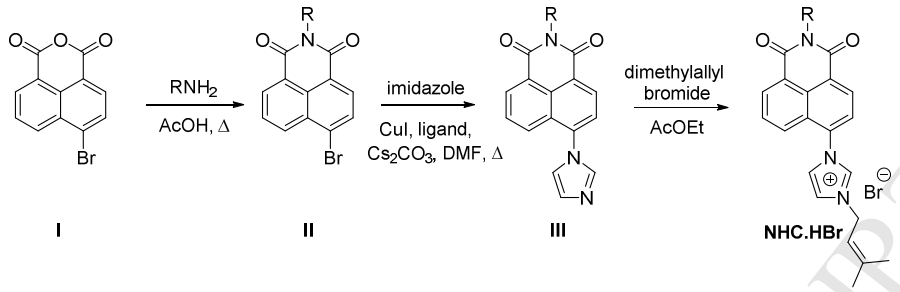

Scheme 1. Synthesis of imidazolium bromide salt **NHC.HBr**, precursor of complexes **1** and **2** (R = 2,6-diisopropylphenyl, ligand = (*S*)-(*N*-benzylpyrrolidin-2-yl)-2-methylimidazole).

The desired Pd(II) NHC complexes were synthesized in good yields using a well-established procedure (Scheme 2), via generation of carbene *in situ* from the relevant imidazolium salt by a weak base in the presence of corresponding dimeric palladacycles [45, 46].

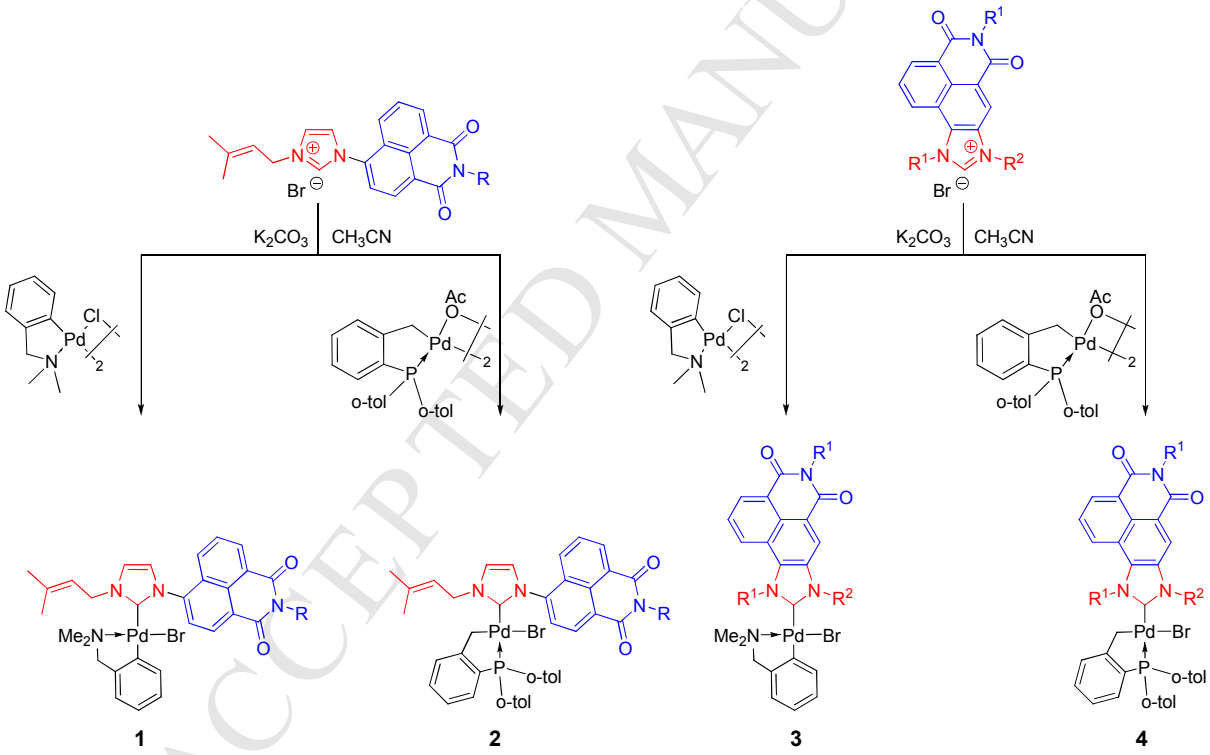

Scheme 2. Synthesis of Pd(II) NHC complexes (R = 2,6-diisopropylphenyl, R^1 = n-butyl, R^2 = 4-methylbenzyl, o-tol = *ortho*-tolyl).

Conformations and Exchange Mechanisms of Complexes 1-4 (Fluxional Behavior and Solution Structure of complexes 1-4)

The structures of the newly synthesized complexes **1-4** were confirmed by 1D and 2D NMR spectra. Conformational exchanges occurred in solution at rates that were intermediate on the NMR time scale. For complexes **1**, **2** and **4** the signals were broad at room temperature and therefore, it was necessary to measure NMR spectra at lower

temperatures. However, the spectra of complex **3** were recorded at room temperature due to the presence of a single preferred conformer.

Four conformers are predictable for *1,3-disubstituted* Pd(II) NHC complexes **1** and **2** (Scheme 3): two conformers due to rotation around the C-N bond and two conformers due to rotation around C-Pd bond. The ^{1}H, ^{13}C and ^{31}P NMR spectra of complex **2** showed the expected four conformers, while the ^{1}H and ^{13}C NMR spectra of complex **1** showed only two conformers. Therefore it can be concluded that restricted rotation around only one of the two possible bonds occurs, while in complex **2** the inversion of phosphine helicity is responsible for additional conformers.

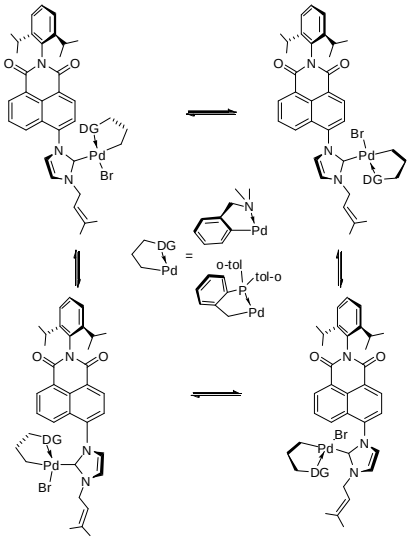

Scheme 3. Possible exchanges in complexes **1** and **2** by rotation around C-N and C-Pd bonds.

The decrease of observed number of conformers in *4,5-fused* Pd(II) NHC complexes **3** and **4** (one and two, respectively) compared to *1,3-disubstituted* Pd(II) NHC complexes **1** and **2** (two and four, respectively) can be explained by the restricted rotation around C-N bond (Figure 2). Further this conclusion was confirmed by comparison of experimental and DFT calculated rotational barriers around C-N and C-Pd bonds.

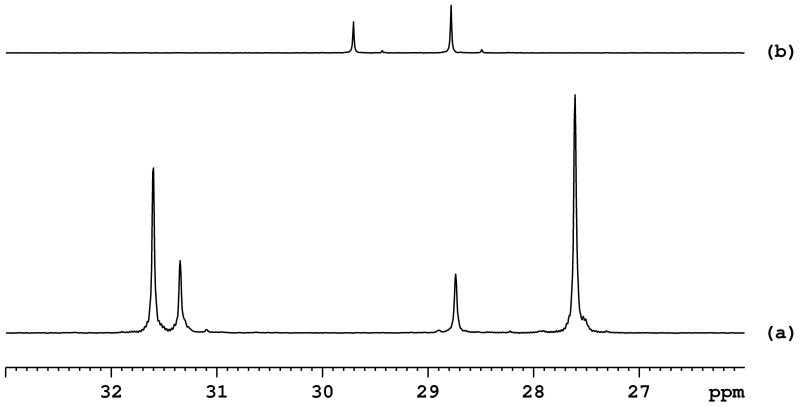

Figure 2. Comparison of ^{31}P NMR spectra of complexes **2** (a) and **4** (b) in $CDCl_3$ at 233 K. Only in the lower spectrum signals due to rotation around C-N bond are observed.

In Scheme 4 the potential diastereomers of complex **2** as viewed down the C-Pd-P bonds are presented. The diastereomers are related horizontally by rotation around C-N amine bond and vertically by inversion of phosphine helicity. The top conformers are right-handed twist (Δ) propellers and bottom conformers are left-handed twist (Λ) propellers. Similar inversion of phosphine helicity is observed in the *4,5-fused* Pd(II) NHC complex **4**.

In order to assign the signals of conformers in NMR spectra we performed DFT and NMR shift calculations for all possible conformers of the complexes. The study of exchange processes between the conformers was performed experimentally by complete line shape analysis (CLSA) of ^{1}H NMR spectra of complex **1**, by ^{31}P EXSY spectra of complexes **2** and **4** and by DFT calculations of the rotation around the C-N and C-Pd bonds of complexes **1** and **2**. The ratio of isomers was determined by signal integration in ^{1}H NMR spectra of complex **1** and ^{31}P VT NMR spectra of complexes **2** and **4** (Table 1). DFT calculated populations fit perfectly to the experimental populations of the conformers in complexes **2** and **4**, while the calculated populations in complexes **1** and **3** only predict the preferred conformer.

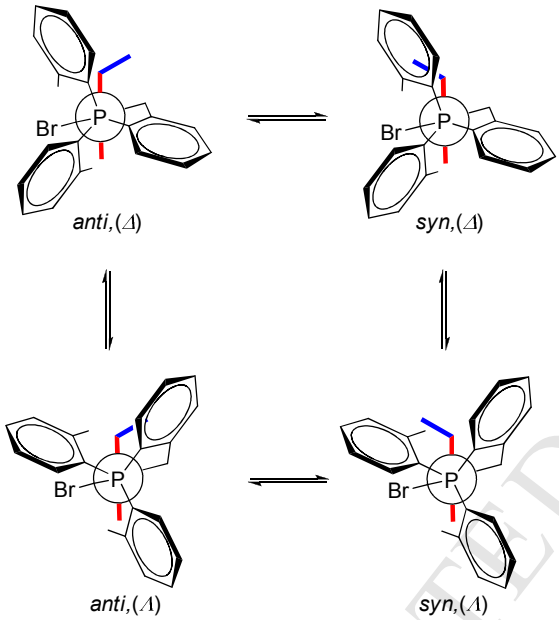

Scheme 4. Potential diastereomers of complex **2** as viewed down the C-Pd-P bond. Diastereomers are related horizontally by rotation around C-N amine bond and vertically by inversion of phosphine helicity.

Table 1. Comparison of experimental and calculated populations of the conformers.

Conformer	ΔG difference (kcal) [a]	Calc. populations (%) [a]	Exp. populations (%) [b]
1-*anti*	0	99.7	52.4
1-*syn*	2.5	0.3	47.6
2-*anti*,(Δ)	0	47	47
2-*anti*,(Λ)	0.2	31	30
2-*syn*,(Λ)	0.4	17	13
2-*syn*,(Δ)	0.9	5	9
3-*anti*	0	90	100
3-*syn*	1.3	10	n.o.
4-(Δ)	0.4	33	33
4-(Λ)	0	67	67

[a] Calculated by the DFT method at B3LYP/ECP (LanL2DZ for Pd and 6-31G* for other atoms) level of theory at 223 K for complex **1**, at 213 K for complex **2** and at 243 K for complex **4**.

[b] Calculated by integration of experimental ^{1}H NMR spectrum at 223 K for complex **1**, by integration of ^{31}P NMR spectrum at 213 K for complex **2** and at 243 K for complex **4**. n.o.: not observed

The assignment of the signals in ^{1}H NMR spectra to particular conformer was confirmed by NMR shift calculations. The experimental and calculated ^{1}H chemical shifts of *syn*- and *anti*- conformers of complex **1** for naphthalimide protons 4-H, 5-H and 7-H (for proton numbering see Supp. Info), which are most sensitive to exchange, are presented in Table 2 and a very good agreement between the calculated and observed ^{1}H chemical shifts was found. Selective experimental and calculated ^{1}H chemical shifts of possible conformers of complex **3** are also given in the Table 2 in order to estimate the errors in NMR shift prediction at the chosen level of theory. The attempt to confirm the assignment of the conformers of complexes **2** and **4** by NMR shift calculations was obstructed by the very small difference in either ^{1}H (Table 2) or ^{31}P (see exp. part) chemical shifts of conformers. The difference in conformers chemical shifts were of order of expected errors in chemical shift prediction, which prevents additional confirmation of conformers assignment. The assignment of the signals in ^{1}H NMR spectrum of complex **4** in aromatic region of phosphine moiety was accomplished using ^{31}P-^{1}H HMBC correlation (Fig. 3).

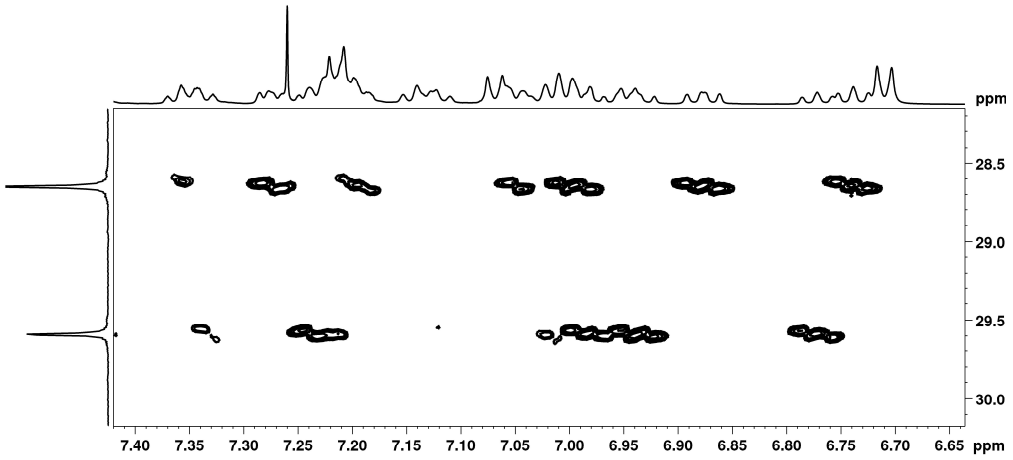

Figure 3. ^{31}P-^{1}H HMBC spectrum for complex **4** in $CDCl_3$ at 233 K, the correlation involves aromatic protons in phosphine moiety.

Table 2. Selected experimental and calculated ^{1}H chemical shifts using B3LYP/ECP (LanL2DZ for Pd and 6-31G(d) for other atoms) geometries in ppm. [a]

Conformer	1-H Exp./calc.	2-H Exp./calc.	3-H Exp./calc.	4-H Exp./calc.	5-H Exp./calc.	7-H Exp./calc.	8-H Exp./calc.	9-H Exp./calc.
1-*anti*				9.33/9.35	10.11/10.07	8.30/8.19	7.98/7.75	9.17/9.07
1-*syn*				8.95/8.91	7.54/7.53	10.22/10.05	8.27/8.12	9.13/9.15
2-*anti*,(*Λ*)				8.26/9.05	8.76/9.64			
2-*syn*,(*Λ*)				8.62/8.82	7.95/8.39			
2-*syn*,(*Δ*)				8.52/8.82	7.69/7.77			
2-*anti*,(*Δ*)				8.61/8.92	8.70/9.35			
3-*anti*	8.64/8.92	7.94/8.20	8.68/8.97			8.56/8.87		
3-*syn*	n.o./8.92	n.o./8.28	n.o./8.96			n.o./8.61		
4-(*Δ*)	8.59/8.90	7.98/8.21	8.70/8.93			8.70/8.93		
4-(*Λ*)	8.53/8.99	7.93/8.27	8.66/8.93			8.68/8.87		

[a] Experimental ^{1}H NMR chemical shifts are measured at -50°C for complexes **1** and **2**, -40°C for complex **4**, while for complex **3** the reported values are at room temperature. The PCM//B3LYP/ECP (LanL2DZ for Pd and 6-31G(d) for other atoms) calculated ^{1}H NMR chemical shifts use TMS as a reference system. n.o.: not observed

Further refinements of the assignment were based on the observed exchange peaks in the ^{31}P EXSY spectra of complex **2**. Exchange peaks in the ^{31}P EXSY spectrum of **2** (Fig. 4) are observed only between *anti* and *syn*

conformers, and between (*Λ*) (left-handed twist) and (*Δ*) (right-handed twist) conformers, as well. This is in agreement with the assignment of the conformers.

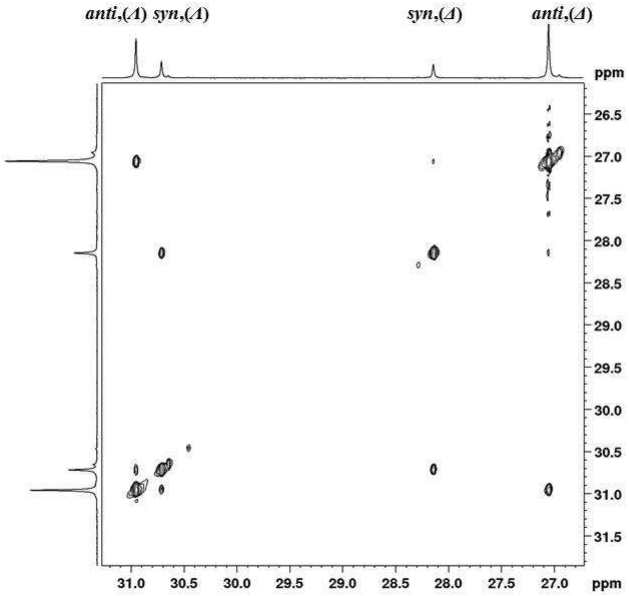

Figure 4. ^{31}P EXSY spectrum of complex **2** in $CDCl_3$ at 243 K using mixing time of 0.1 s.

It is well known that in metal complexes from the second and the third transition series, the values of vicinal coupling constants depend strongly on the geometry and $^2J(^{31}\text{P-M-L}_{trans}) > {}^2J(^{31}\text{P-M-L}_{cis})$ [47]. For the directly bound σ carbon, the same geometric dependence of ^2J(P,C) is observed, for example for organometallic chiral complexes of palladium containing the chelate Duphos, $^2J(\text{P,C})_{trans}$ = *ca*. 101, $^2J(\text{P,C})_{cis}$ = *ca*. 5 Hz [48]. Therefore our experimental values for $^2J(\text{C}_{\text{carbene}}\text{-Pd-P})$ (144.5 Hz for major conformer of complex **2** and 142.0 Hz for both conformers of complex **4**) prove the *P*-donor ligand's *trans* orientation in respect to the carbene atom.

*Analysis of the variable temperature 1D ^{1}H NMR spectra of Pd complex **1** and DFT calculations of Pd complex **1***

The dynamic NMR study of Pd complex **1** was carried out in $CDCl_3$ in the temperature range from 223 K to 328 K. The low temperature ^{1}H NMR spectrum of **1** exhibits two resonances for each nonequivalent proton. These resonances correspond to two conformers with of 1.0 : 1.1 integral ratio at 223 K. The Complete Line Shape Analysis (CLSA) of the aromatic protons in the range from 7.5 to 9.5 ppm was performed. The ^{1}H NMR measured and fitted signals of aromatic protons of complex **1** in $CDCl_3$ at different temperatures and the corresponding rate constants are presented in Fig. 5. The NOESY spectrum of complex **1** in $CDCl_3$ at 278 K using mixing time of 1.0 s is presented on Fig. 2S and the five exchanging pairs are clearly seen. The difference between the chemical shift of exchanging sites are in the range between 0.1 and 1.4 ppm. They coalesce at different temperatures, thus effectively increasing the temperature range in which the lineshape is most sensitive to the rate constant changes. Therefore it is not surprising to achieve a very good linear dependence of the rate constants in Eyring plots, as evidenced by correlation coefficients ranging from 0.9980 to 0.9985 (Fig. 3S, 13 rate constants in temperature range of 105 K). The activation parameters $\Delta S^{\neq}$, $\Delta H^{\neq}$ and $\Delta G^{\neq}$ at T = 298.2 K are summarized in Table 3.

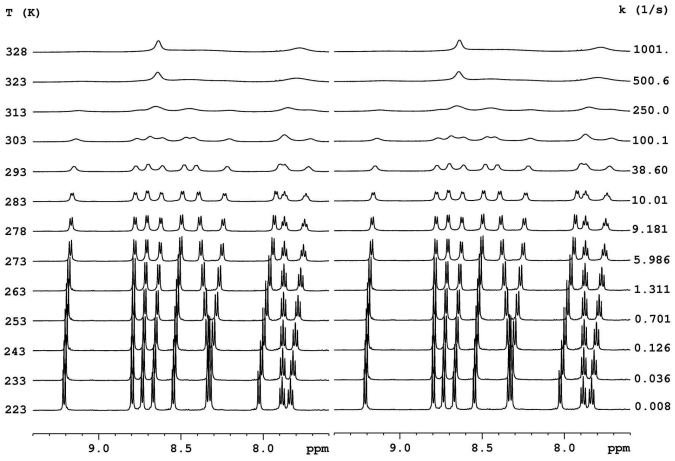

Figure 5. Measured (left) and calculated (right) ^{1}H NMR spectra of the aromatic protons in complex **1** in $CDCl_3$ at different temperatures and the corresponding rate constants.

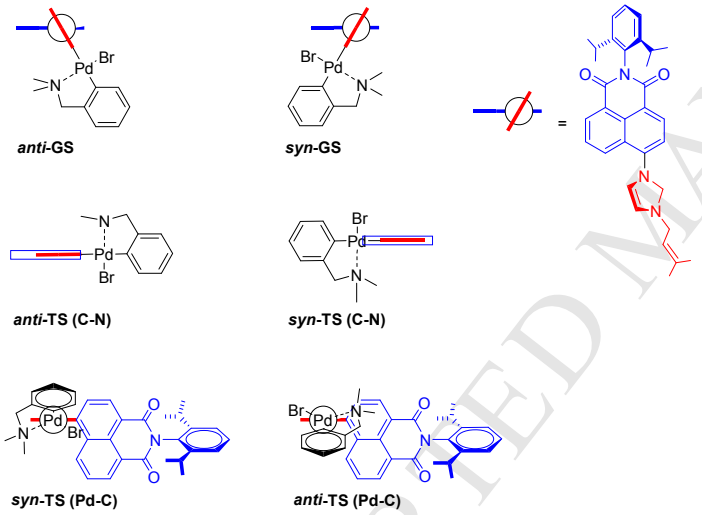

Figure 6. The calculated ground state (GS) and transition state (TS) conformers of complex **1**.

In order to find out which are the preferred stable conformers and to model the possible transition structures, DFT calculations of Pd complex **1** were carried out. Two ground state (GS) structures and two sets of transition state (TS) structures were localized computationally (Fig. 6). The *anti*-GS (Br atom is *anti* in respect to naphthalimide) is energetically preferred compared to *syn*-GS. Therefore, the assignment of the *major* conformer as *anti*-GS and *minor* as *syn*-GS can be made, which is in agreement with the results from NMR shift calculations for imidazole protons 4-H, 5-H and 7-H, presented in Table 2.

For the rotation around C-N bond two TS were located: *anti*-TS (Pd atom is *anti* in respect to naphthalimide) and *syn*-TS. The *anti*-TS is lower in energy than the *syn*-TS. For the rotation around C-Pd bond two TS were located, as well: *anti*-TS (Br atom is *anti* in respect to naphthalimide) and *syn*-TS (Br atom is *syn* in respect to naphthalimide). The *anti*-TS is lower in energy than the *syn*-TS.

The calculated rotational barriers for rotation around C-N and Pd-C bond are summarized in Table 3. There is a good agreement between the experimental free energy and the calculated one for the C-N rotation. Therefore the observed conformers are due to the restricted rotation around C-N bond, which is in agreement with the experimental observations (Fig. 2).

Table 3. Standard activation parameters for the rotational barriers of complex **1**.

Method	$\Delta H^{\neq}$ (kcal mol^{-1})	$\Delta S^{\neq}$ (cal K^{-1} mol^{-1})	$\Delta G^{\neq}$ (kcal mol^{-1})	$\Delta G^{\neq eff}$ (kcal mol^{-1})
Pd-C rotation: [a]				
syn-TS (Pd-C) - *anti*-GS	23.2	-2.7	24.0	
anti-TS (Pd-C) - *anti*-GS	23.0	-4.2	24.3	23.7
N-C rotation: [a]				
syn-TS (C-N) - *anti*-GS	17.4	-8.3	19.8	
anti-TS (C-N) - *anti*-GS	14.5	-8.6	17.1	17.1
NMR experiment *major* to *minor*	15.4 ± 0.3	1.6 ± 1.0		14.97 ± 0.13
Pd-C rotation: [a]				
syn-TS (Pd-C) - *syn*-GS	20.9	-1.0	21.2	
anti-TS (Pd-C) - *syn*-GS	20.8	-2.4	21.5	20.9
N-C rotation: [a]				
syn-TS (C-N) - *syn*-GS	15.1	-6.6	17.1	
anti-TS (C-N) - *syn*-GS	12.3	-6.9	14.3	14.3
NMR experiment *minor* to *major*	15.2 ± 0.4	0.6 ± 1.0		15.05 ± 0.14

[a] ZPE, thermal and entropy corrections are calculated at PCM//B3LYP/ECP (LanL2DZ for Pd and 6-31G* for other atoms) level of theory for 298 K.

*Analysis of the variable temperature 2D ^{31}P EXSY NMR spectra of Pd complex **2** and DFT calculations of complex **2***

The dynamic NMR study of Pd complex **2** was carried out in $CDCl_3$ by measuring NMR spectra in the temperature range of 213 K to 328 K. The low temperature ^{1}H and ^{31}P NMR spectra of **1** exhibit four resonances for every nonequivalent nucleus. The ^{31}P NMR resonances at 31.57, 31.28, 28.53 and 27.29 ppm correspond to four conformers with integral ratio 1.0 : 0.44 : 0.30 : 1.56 at 213 K. In Fig. 3 the ^{31}P EXSY spectrum of **2** in $CDCl_3$ at 243 K using mixing time of 0.1 s is presented. The assignment of the conformers is based on the very good agreement between experimental and calculated populations of the conformers of complex **2** (Table 1) and by observation of exchange peaks in the ^{31}P EXSY spectrum of **2** (Fig. 3) only between *anti* and *syn* conformers, and only between (Λ) (left-handed twist) and (Δ) (right-handed twist) conformers, as well.

The peak volume integration of ^{31}P EXSY spectra of complex **2** in $CDCl_3$ in the temperature region between 223 K and 253 K was carried out and the calculated rate constants are presented in Table 4S. The activation parameters of the studied exchanges of complex **2** are summarized in Table 5S. The Eyring plots demonstrate a very good linear dependence of the rate constants, as evidenced by high correlation coefficients ranging from 0.9986 to 0.9999 (Fig. 5S, 7 rate constants in temperature range of 30 K).

The starting geometries for DFT studies of the four conformers of complex **2** were prepared starting from X-ray data of $Pd_2(\mu\text{-}OAc)_2\{o\text{-}CH_2C_6H_4P(o\text{-}Tol)_2\}_2$ structure [49]. Similarly to complex **1** two GS of **2** were studied computationally (Fig. 7). The *anti*-GS(Δ) (Br atom is *anti* in respect to naphthalimide) is energetically preferred compared to *syn*-GS(Δ). For the rotation around C-N bond two TS were located: *anti*-TS (Pd atom is *anti* in respect to naphthalimide) and *syn*-TS (Pd atom is *syn* in respect to naphthalimide). The *anti*-TS is lower in energy than the *syn*-TS. For the rotation about C-Pd bond two TS were located, as well: *anti*-TS (Br atom is *anti* in respect to naphthalimide) and *syn*-TS (Br atom is *syn* in respect to naphthalimide). The *anti*-TS is lower in energy than the *syn*-TS.

The experimental and theoretical activation parameters for the rotational barriers of complex **2** are summarized in Table 4. Similar to complex **1**, it is clearly seen that the C-N restricted rotation is the process, which we observe in NMR spectra. There is a good agreement between the experimental free energy and the calculated one for the C-N rotation.

Molecular propellers and gears as artificial molecular rotors were reviewed recently [50]. Mislow and co-workers performed the first detailed investigation of correlated rotation in aryl propeller systems [51]. For three phenyl propellers four ring-flip mechanisms are possible. The mechanism of correlated rotations in phosphorus analogues of triarylmethanes were studied using iterative analysis of exchange-broadened NMR band shapes by Binsch and co-workers [52]. The lowest energy process for P-C bond rotation in P(*o*-tol)$_3$ complexes involves rotation of one ring through the plane perpendicular to the M-P-*ipso*-C plane with correlated rotation of the other two rings through the corresponding M-P-*ipso*-C planes [53, 54]. This two-ring-flip mechanism [55, 56] leads to complete interchange of the *o*-tolyl rings. The mechanism and dynamic stereochemistry of Pd{2-$CH_2C_6H_4$P(*o*-tol)$_2$} propeller has not been studied yet. The bridging bonding reduces the flexibility of 2-$CH_2C_6H_4$ ring and it is difficult to predict which will be the preferred mechanism of interconversion without detailed DFT study of all possible ring-flip mechanisms. Such study can only be performed using enormous computer resources on a much smaller model complex and is out of the scope of this investigation.

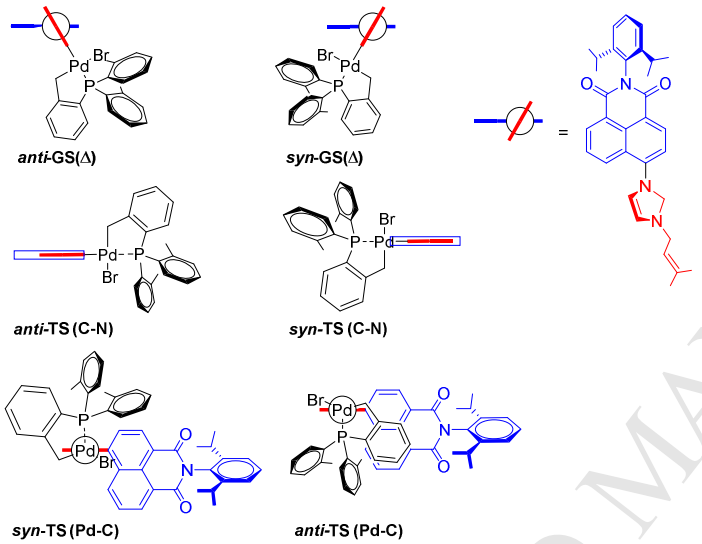

Figure 7. The calculated ground state (GS) and transition state (TS) conformers of complex **2**. All TS in figure are (Δ) (right-handed twist) propeller structures.

Table 4. Standard activation parameters for the rotational barriers of complex **2**.

Method	$\Delta H^{\neq}$ (kcal mol^{-1})	$\Delta S^{\neq}$ (cal K^{-1} mol^{-1})	$\Delta G^{\neq}$ (kcal mol^{-1})	$\Delta G^{\neq eff}$ (kcal mol^{-1})
Pd-C rotation: [a]				
syn-TS (Pd-C) - *anti*-GS	23.1	-6.6	25.1	
anti-TS (Pd-C) - *anti*-GS	18.5	-2.3	19.2	19.2
N-C rotation: [a]				
syn-TS (C-N) - *anti*-GS	20.2	-3.0	21.1	
anti-TS (C-N) - *anti*-GS	14.8	-5.1	16.4	16.4
NMR experiment *anti*,(*Δ*) to *syn*,(*Δ*)	13.9 ± 0.6	-4.8 ± 2.9		15.36 ± 0.07
Pd-C rotation: [a]				
syn-TS (Pd-C) - *syn*-GS	21.8	-7.7	24.1	
anti-TS (Pd-C) - *syn*-GS	17.3	-3.4	18.3	18.3
N-C rotation: [a]				
syn-TS (C-N) - *syn*-GS	18.9	-4.0	20.1	
anti-TS (C-N) - *syn*-GS	13.6	-6.2	15.4	15.4
NMR experiment *syn*,(*Δ*) to *anti*,(*Δ*)	12.2 ± 0.6	-9.3 ± 2.6		14.99 ± 0.07

[a] ZPE, thermal and entropy corrections are calculated at PCM//B3LYP/ECP (LanL2DZ for Pd and 6-31G* for other atoms) level of theory for 298 K. All GS and TS in table are (Δ) (right-handed twist) propeller structures.

*Analysis of the variable temperature 2D ^{31}P EXSY NMR spectra of Pd complex **4***

The dynamic NMR study of Pd complex **4** was carried out in $CDCl_3$ in the temperature range from 233 K to 323 K. The low temperature ^{1}H and ^{31}P NMR spectra of **1** exhibit two resonances for every nonequivalent nucleus. The ^{31}P NMR resonances at 29.70 and 28.78 ppm correspond to two conformers with 1.0 : 1.59 integral ratio at 233 K (Similar integral ratio is observed between *anti*,(*Λ*) and *anti*,(*Δ*) conformers of complex **2**). In the Fig. 7S the ^{31}P EXSY spectrum of complex **4** in $CDCl_3$ at 233 K using mixing time of 1.3 s is presented.

The peak volume integration of ^{31}P EXSY spectra of complex **4** in $CDCl_3$ in the temperature region between 233 K and 283 K was carried out and the calculated rate constants are presented in Table 5S. The activation parameters of the studied exchanges of complex **4** are summarized in Table 7S. The Eyring plots demonstrate a very good linear dependence of the rate constants, as evidenced by very high correlation coefficients (higher than 0.9999, Fig. 8S, 7 rate constants in temperature range of 50 K).

It is worth to note that all studied exchange barriers are in the short range between 14.0 and 15.4 kcal/mol (Tables 3, 4, 5S and 7S) thus making the assignment of NMR spectra difficult without combination of dynamic NMR study and DFT calculation. The applied integrated approach, which combines methods of dynamic NMR spectroscopy and computational chemistry, was successful in estimation the stability of conformers, in prediction of ^{1}H NMR chemical shifts and in the estimation of rotational barriers. The applied computational approach use moderate basis sets and the B3LYP functional, which is objected to criticism because this functional do not describe pure dispersion interactions [57]. We managed to solve the problems of assignment of conformers and reveal the exchange mechanism at the possible reasonable computational cost.

On the other hand the fact that the studied barriers are of the same order (14.0 ÷ 15.4 kcal/mol) may be connected with the same origin of the studied restricted fluxional motions. Similar steric factors may influence these fluxional motions. In 1,3-nonsubstituted Pd-NHC complexes DFT calculations predict energy barriers around the Pd−NHC bond of 3.0 and 4.9 kcal/mol [58]. In bis Pd-NHC complexes with unsymmetrical 1,3-substituents the energy barrier around Pd−NHC bond of 17.7 kcal/mol was estimated using the coalescent method [59]. The rotational barriers of mesityl rings around C-N bonds in Ru-NHC complexes were estimated to be in the range of 14.5 ÷ 15.5 kcal/mol depending of solvent [60]. At the same time the rotational barrier around the C–N bond in simple *N*,*N*-dimethylaniline has been calculated to be 5.1 kcal/mol [61]. The resonance contribution can be neglected for C-N rotation in *1,3-disubstituted* Pd(II) NHC complexes **1** and **2** since the two aromatic systems (naphthalimide and NHC) are not coplanar. Therefore the steric hindrance that occurs between the Pd ligands and 1- and 3- substituents in NHC are mainly responsible for the increased barriers of studied restricted fluxional motions.

Catalytic activity of complexes 3 and 4

The catalytic activity of complex **3** and **4** was studied in Suzuki-Miyaura reactions, using 4-bromoanisole and phenylboronic acid as model reagents, due to its fertility for preparation of wide range of unsymmetrical biaryls, low toxicity and usage of mild conditions, compared to other cross-coupling reactions. The reaction is tolerant of a wide range of functional groups, and the nature of the initial precatalyst, solvent and base are crucial for excellent yields.

Preliminary experiments were performed with complexes **3** and **4**, using low catalyst loading (0.1 mol %, Scheme 5). Complex **3** exhibited higher activity: the yield obtained by this precatalyst was 35 % vs. 27 % for the phosphorus counterpart **4**.

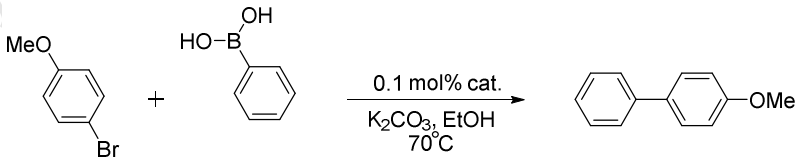

Scheme 5.

Complex **3** was chosen for optimization of the reaction conditions. Reactions were performed in 0.1 mmol scale. The yields were determined using ^{1}H NMR spectra with ferrocene as an internal standard. Solvent screening was examined with potassium carbonate as base and representative results are summarized in Table 5. The highest yields were obtained with dimethoxyethane/water mixture (5:1) and toluene under inert atmosphere in both cases, therefore both of them were used for base screening.

Table 5. Solvent screening in Suzuki-Miyaura reaction.[a]

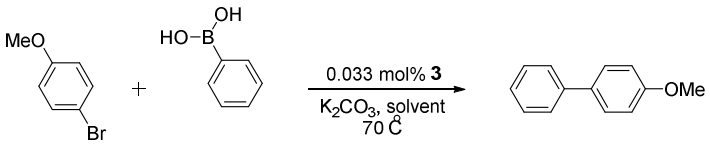

Entry	Solvent	Conditions	Yield (%)
1	Water	argon	6
2	DME	argon	8
3	DME-H_2O, 5:1	argon	72
4	Dioxane	argon	7
5	Dioxane-H_2O, 5:1	argon	42
6	CH_3CN	argon	19
7	CH_3CN-H_2O, 5:1	argon	10
8	Isopropyl alcohol	argon	7
9	Ethanol	air	7
10	Ethanol	argon	29
11	toluene	argon	82
12	THF	argon	9

[a] Reaction conditions: 4-bromoanisole (0.1 mmol), phenylboronic acid (1.2 equiv.), K_2CO_3 (3 equiv.), complex **3** (0.033 mol%), solvent (0.6 mL), 12 h.

Due to importance of the base in Suzuki-Miyaura reaction, screening was performed using the most frequently reported in the literature bases (Table 6). The best results were obtained in dimethoxyethane/water mixture with potassium phosphate as base, besides toluene with potassium carbonate.

Table 6. Base screening in Suzuki-Miyaura reaction.[a]

Entry	Solvent	Base	Yield (%)
1	DME-H_2O, 5:1	K_2CO_3	7
2	Toluene	K_2CO_3	83
3	Toluene-H_2O, 5:1	K_2CO_3	7
4	Ethylene glycol	K_2CO_3	27
5	DME-H_2O, 5:1[b]	K_2CO_3	7
6	DME-H_2O, 5:1	Cs_2CO_3	7
7	DME-H_2O, 5:1	CsF	4
8	DME-H_2O, 5:1	K_3PO_4	85
9	DME-H_2O, 5:1	$Ba(OH)_2$	5
10	Toluene	K_3PO_4	66
11	Toluene-H_2O, 7:1	K_3PO_4	66

[a] Reaction conditions: 4-bromoanisole (0.1 mmol), phenylboronic acid (1.2 equiv.), K_2CO_3 (3 equiv.), complex **3** (0.033 mol%), solvent (0.6 mL), reflux, 12 h, under argon.

[b] with complex **4**;

After reaction conditions optimization, the catalytic activity of both carbene complexes was compared once more. Toluene was preferred as a solvent, because of its higher boiling point and less irritating properties. In this case, preparative experiments in 1 mmol scale of 4-bromoanisole were performed and the quantity of catalyst was increased to 0.066 mol %, the amount of phenylboronic acid was slightly increased to 1.5 equiv, and the reaction was performed under inert atmosphere by refluxing for 12 h. Both catalysts showed high activity, yielding 4-methoxybiphenyl in 95 % isolated after flash chromatography (cyclohexane : dichloromethane = 24 : 1).

3. Conclusion

In conclusion, we have synthesized four new NHC complexes involving bidentate *N*- and *P*-donor ligands. Conformational studies in respect of hindered rotation around C-N bond, Pd-C and phosphine helicity were performed. The conformations of the newly prepared complexes were elucidated on the base of NMR and DFT studies. In solution of *1,3-disubstituted* complex **1** two conformers were revealed and proved to originate from restricted rotation around C-N bond, while for *1,3-disubstituted* complex **2** four conformers resulting from the restricted rotation around C-N bond and phosphine helicity reversal were observed. In the case of *4,5-fused* complex **3** only one conformer was detected, while for *4,5-fused* complex **4** two conformers resulting from phosphine helicity reversal were observed. The palladium complexes **3** and **4** were evaluated as catalysts in Suzuki–Miyaura Reaction and exhibited excellent catalytic activity.

4. Experimental section

4.1. General

All reagents purchased from commercial suppliers were used without any further purification. 6-bromo-2-(2,6-diisopropylphenyl)-1*H*-benzo[*de*]isoquinoline-1,3(2*H*)-dione, (*S*)-1-((1-Benzylpyrrolidin-2-yl)methyl)-2-methyl-1H-imidazole, 10-dibutylbenzo[*de*]imidazo[4,5-*g*]isoquinoline-4,6(5*H*,10*H*)-dione and *trans*-di(μ-acetato)-bis[*o*-(di-*o*-tolylphosphino)benzyl]dipalladium(II) were synthesized using published procedures [43, 44, 62, 63]. All of the reactions were performed under inert atmosphere using standard Schlenk techniques. The NMR spectra were recorded on a Bruker Avance II+ 600 (600.13 for ^{1}H NMR, 150.92 MHz for ^{13}C NMR and 242.92 MHz for ^{31}P NMR) spectrometer with TMS (85% H_3PO_4 for ^{31}P) as internal standard for chemical shifts (δ, ppm). ^{1}H and ^{13}C NMR data are reported as follows: chemical shift, multiplicity (s = singlet, d = doublet, t = triplet, q = quartet, br = broad, m = multiplet), coupling constants *J* (Hz), integration and identification. The assignment of the ^{1}H and ^{13}C NMR spectra was made on the basis of DEPT, COSY, HSQC, HMBC and NOESY experiments. Flash chromatography was performed on Silica Gel 60 (0.040–0.063 nm). Elemental analyses were performed using Vario EL*3* CHNS(O) and Microanalytical service Laboratory of the Institute of Organic Chemistry, Bulgarian Academy of Science.

4.2. Dynamic NMR measurements

VT ^{1}H NMR spectra of complex **1** were recorded on a Bruker II+ 600 instrument (BBO probe) at 600.13 MHz in steps of 10 K between 223 and 323 K in $CDCl_3$. VT ^{1}H and ^{31}P{^{1}H} (power-gated decoupling of ^{1}H) spectra of complex **2** were recorded at 600.13 MHz and 242.94 MHz in steps of 5 K between 213 and 323 K in $CDCl_3$, for complex **4** between 233 and 323 K. Temperature calibration was done with B-VT 3000 unit (it was checked and calibrated with methanol and ethylene glycol reference samples). ^{1}H NMR spectra were acquired using a spectral width of 10 kHz, an acquisition time of 3.4 s and 32 scans, zerofilled to 64k datapoints (0.15 Hz per point) and processed without apodization.

The Complete Line Shape Analysis of exchange broadened spectra of complex **1** was performed by the dnmr module of topspin suite of programs. The chemical shifts and populations were obtained by lorenzian fit at lower temperatures and extrapolated to higher temperatures. The signal of TMS was used as a reference and the following equation was used to estimate the T_2 values of the exchanging signals: $T_2 = 1/[\pi(W_{ref} + \Delta W)]$, where $\Delta W = W_0 - W_{ref}$, ΔW is the difference between the halfwidth of the reference signal, W_{ref}, and the observed signal in the absence of exchange, W_0 [64]. In the fitting procedure, all parameters were allowed to change and the overlap of more than 95% was achieved. The rate constant of the process *major* to *minor* conformers was fitted, while the other was recalculated using the populations ratio.

VT ^{1}H EXSY NMR spectra of compounds **1**–**4** were recorded on a Bruker II+ 600 instrument (BBO probe). The spectra were acquired using a spectral width of 1.2 kHz, 2048 x 256 complex time domain datapoints, with 2 scans in

about 45 min. The spectra were zerofilled to 4096 x 4096 datapoints and processed with a shifted square sine bell apodization in both dimensions.

VT ^{31}P EXSY spectra (power-gated decoupling of ^{1}H) of complex **2** were recorded on a BBO probe in steps of 5 K between 223 and 253 K, for complex **4** between 233 and 283 K**.** The spectra were acquired using a spectral width of 4.8 kHz, 2048 x 256 complex time domain data points, mixing times in the range of 0.075 to 1.0 s and 2 scans in about 45 min. Linear prediction (32 coefficients and 256 points) in F1 was applied. The spectra were zerofilled to 4096 x 4096 data points and processed with a shifted square sine bell apodization in both dimensions. The populations were obtained by integration of 1D ^{31}P signals and the exchange rates were calculated by program EXSYCalc [65] from diagonal- and crosspeak integrals.

The errors E_{tot}, quoted in Tables 3, 4, 2S, 5S and 7S are calculated according to the expression: $E_{tot} = \sqrt{E_S^2 + E_{kT}^2}$, where E_S is the statistical error based on scattering of the data in the Eyring plot while E_{kT} is computed using error propagation equations as derived by Binsch [66] and Heinzer and Oth [67], in which errors due to both the calculated rate constants and the measured temperature are taken into account. The absolute error in temperature is assumed to be not more than ±0.5 K. The relative errors in *k* are estimated to be not more than ±10% at all temperatures according the precision of the volume integration of peaks. The errors analysis was performed using a self-made computer program using the cited equations.

4.3. DFT calculations

Geometry optimizations were performed by using the density functional theory [68-70] as implemented in GAUSSIAN 09 [71] and the B3LYP functional [72, 73]. As for the basis sets, we used 6-31G(d) for C, H, P and Br [73]. For Pd, the basis set LANL2DZ was adopted [74], whose core parts were represented by effective core potentials (ECP). Solvent was included implicitly to the optimizations via the SMD [75] model with the built in parameters for solvent $CHCl_3$. After locating the first GS structure, the next one was found by scanning the torsional profile for the rotation (incrementing the dihedral angle about C-N or Pd-C bond in 10 degrees step). The next minimum on the torsional profile was fully optimized in order to locate the next GS structure. The maximum in the reaction coordinate calculations was optimized by fixing the dihedral angle of rotation and subsequent full geometry optimization of the TS structure using the Berny algorithm. All critical points (GS and TS structures) were characterized by performing vibrational analysis, and ZPV energies were also evaluated. The thermal and entropy corrections to the Gibbs free energy at 298.15 K were calculated for all minima using unscaled vibrational frequencies obtained at the same level.

The ^{1}H NMR chemical shifts of complexes in chloroform environment (SMD) were calculated using the B3LYP functional with the 6-31+G(d,p) basis set for C, H, P and Br [73]. For Pd, we used LANL2DZ basis set [74], whose core parts were represented by effective core potentials (ECP).

4.4. **2-[2,6-di(propan-2-yl)phenyl]-6-(1H-imidazol-1-yl)-1H-benzo[de]isoquinoline-1,3(2H)-dione** (**III**): 6-bromo-2-(2,6-diisopropylphenyl)-1H-benzo[*de*]isoquinoline-1,3(2*H*)-dione (**II**) (2.00 g, 4.5 mmol), CuI (0.044 g, 0.23 mmol, 5 mol %), (*S*)-1-((1-Benzylpyrrolidin-2-yl)methyl)-2-methyl-1H-imidazole (0.116 g, 0.45 mmol 10 mol%), imidazole (0.31 g, 4.5 mmol) and Cs_2CO_3 (2.93 g, 9 mmol) were dissolved in dry DMF (50 mL), degassed and the reaction mixture was heated to 100 °C for 24 hours. The reaction mixture was then poured into water and extracted with $CHCl_3$. The combined organic layers were washed with water, dried with Na_2SO_4 and evaporated. The desired product was isolated by flash chromatography (EtOAc : hexanes = 4 : 1) to give 1.81 g (95% yield) of **III** as a white solid; m.p. 140-142°C. ^{1}H NMR (600 MHz, $CDCl_3$): δ = 1.189 (d, *J* = 6.8 Hz, 12H, $(\mathbf{CH_3})_2$CH), 2.757 (septet, *J* = 6.8 Hz, 2H, $(CH_3)_2$**CH**), 7.374 (d, *J* = 7.7 Hz, 2H, H3, 5-phenyl), 7.432 (bs, 1H, H-imidazole), 7.491 (bs, 1H, H-imidazole), 7.524 (t, *J* = 7.7 Hz, 1H, H4-phenyl), 7.853 (d, *J* = 7.6 Hz, 1H, H5-naphthyl), 7.925 (dd, *J* = 8.5, 7.5 Hz, 1H, H8-naphthyl), 8.164 (d, *J* = 8.6 Hz, 1H, H7-naphthyl), 8.184 (bs, 1H, N**CH**N-imidazole), 8.803(d, *J* = 7.4 Hz, 1H, H9-naphthyl), 8.791 (d, *J* = 7.6 Hz, 1H, H4-naphthyl). ^{13}C NMR (151 MHz, $CDCl_3$): δ = 24.00 (CH$\mathbf{(CH3)_2}$), 29.23 (**CH**$(CH3)_2$), 121.73 (Ar-^{4}C), 123.26 (Ar-^{4}C), 123.45 (Ar-^{4}C), 124.17 (Ar), 124.49 (Ar), 127.68 (Ar-^{4}C), 128.74 (Ar), 128.83 (Ar), 129.35 (N**C**HN), 129.74 (Ar-^{4}C), 129.79 (Ar), 130.36 (Ar-^{4}C), 131.56 (Ar), 132.81 (Ar), 137.91 (Ar-^{4}C), 138.85 (Ar-^{4}C), 145.56 (Ar-^{4}C), 163.20 (^{4}C-carbonyl), 163.70 (^{4}C-carbonyl). $C_{27}H_{25}N_3O_2$ (423.51): calcd. C 76.57, H 5.95, N 9.92, found: C 76.69, H 6.01, N 9.98.

4.5. **1-[2-(2,6-Isopropylphenyl)-1,3-dioxo-2,3-dihydro-1*H*-benzo[*de*]isoquinolin-6-yl]-3-(3-methylbut-2-en-1-yl)-1*H*-imidazol-3-ium bromide**, (**NHC.HBr**, precursor of **1** and **2**): Compound **III** (0.105 g, 0.133 mmol) was dissolved in minimal amount of ethyl acetate and 2,2-dimethylallylbromide (0.04 mL) was added to the resulting

solution. The reaction mixture was stirred at room temperature overnight, then all volatiles were evaporated *in vacuo*. The solid residue was recrystallized from isopropyl alcohol. Yield: 80% m.p. 199-201°C. ^{1}H NMR (600 MHz, $CDCl_3$): δ = 1.153 (d, J = 6.8 Hz, 12H, (**C**$\mathbf{H_3}$)$_2$CH), 1.946 (s, 3H, **C**$\mathbf{H_3}$-butenyl), 1.988 (s, 3H, **C**$\mathbf{H_3}$-butenyl), 2.708 (septet, J = 6.8 Hz, 2H, (CH$_3$)$_2$**CH**), 5.444 (d, J = 7.4 Hz, 2H, H1-butenyl), 5.768 (t, J = 7.4 Hz, 1H, H2-butenyl), 7.337 (d, J = 7.8 Hz, 2H, H3, 5-phenyl), 7.493 (t, J = 7.8 Hz, 1H, H4-phenyl), 7.632 (bs, 1H, H-imidazole), 7.727 (bs, 1H, H-imidazole), 8.016 (dd, J = 8.4, 7.3 Hz, 1H, H8-naphthyl), 8.307 (dd, J = 0.8, 8.4 Hz, 1H, H7-naphthyl), 8.362 (d, J = 7.7 Hz, 1H, H5-naphthyl), 8.777 (d, J = 7.7 Hz, 1H, H4-naphthyl), 8.795 (dd, J = 0.8, 7.3 Hz, 1H, H9-naphthyl), 10.451 (bs, 1H, N**CH**N-imidazole). ^{13}C NMR (151 MHz, $CDCl_3$): δ = 18.54 (**(C**$\mathbf{H_3}$**)**-butenyl), 23.92 ((**C**$\mathbf{H_3}$)$_2$CH), 23.95 ((**C**$\mathbf{H_3}$)$_2$CH), 25.81 (**(C**$\mathbf{H_3}$**)**-butenyl), 29.17 ((CH$_3$)$_2$**CH**), 50.08 (C1-butenyl), 118.02 (C2-butenyl), 123.30 (Ar-^{4}C), 123.52 (CH-imidazole), 124.15 (CH-imidazole), 124.81 (Ar-^{4}C), 124.83 (C3,5-phenyl), 125.34 (Ar-^{4}C), 126.00 (C7-naphthyl), 126.54 (Ar-^{4}C), 128.08 (C4-phenyl), 129.56 (Ar-^{4}C), 129.82 (C5-naphthyl), 129.88 (C7-naphthyl), 130.07 (Ar-^{4}C), 131.18 (C4-naphthyl), 133.23 (C9-naphthyl), 135.28 (Ar-^{4}C), 138.54 (N**CH**N-imidazole), 145.51 (Ar-^{4}C), 162.72 (^{4}C-carbonyl), 163.27 (^{4}C-carbonyl). $C_{32}H_{34}BrN_3O_2$ (572.54): calcd. C 67.13, H 5.99, N 7.34, found: C 67.22, H 6.07, N 7.39.

4.6. **5,10-Dibutyl-8-(4-methylbenzyl)-4,6-dioxo-4,5,6,10-tetrahydrobenzo[*de*]imidazo[4,5-*g*]isoquinolin-8-ium bromide**, (**NHC.HBr**, precursor of **3** and **4**): Suspension of 5,10-dibutylbenzo[*de*]imidazo[4,5-*g*]isoquinoline-4,6(5*H*,10*H*)-dione (1 g, 2.86 mmol) and 4-methylbenzyl bromide (7.54 ml, 20 equiv.) was stirred for 72 hours at 80°C. After coiling to room temperature, the reaction mixture was filtered and washed with diethyl ether. The residue was purified by column chromatography (gradient elution: first eluting with ethyl acetate, after that eluting with mixture of DCM and methanol = 4.5 : 0.5). Yield 1.4 g (90%); m.p. 216-218 °C. ^{1}H NMR (600 MHz, $CDCl_3$): δ = 0.961 (t, J = 7.4 Hz, 3H, **C**$\mathbf{H_3}$-5-n-butyl), 1.025 (t, J = 7.4 Hz, 3H, **C**$\mathbf{H_3}$-10-n-butyl), 1.391-1.452 (m, 2H, 3-**C**$\mathbf{H_2}$-5-n-butyl), 1.577-1.627 (m, 2H, 3-**C**$\mathbf{H_2}$-10-n-butyl), 1.658-1.709 (m, 2H, 2-**C**$\mathbf{H_2}$-5-n-butyl), 2.176-2.225 (m, 2H, 2-**C**$\mathbf{H_2}$-10-n-butyl), 2.278 (s, 3H, **C**$\mathbf{H_3}$-(4-methylbenzyl)), 4.139-4.165 (m, 2H, 1-**C**$\mathbf{H_2}$-5-n-butyl), 5.167-5.192 (m, 2H, 1-**C**$\mathbf{H_2}$-10-n-butyl), 6.015 (s, 2H, **C**$\mathbf{H_2}$-(4-methylbenzyl)), 7.166 (d, J = 8.0 Hz, 2H, H2, 6-4-methylbenzyl), 7.491 (d, J = 8.0 Hz, 2H, H3,5-4-methylbenzyl), 8.087 (dd, J = 7.5, 8.5 Hz, 1H, H2-naphthyl), 8.673 (dd, J = 0.8, 7.5 Hz, 1H, H1-naphthyl), 8.778 (dd, J = 0.8, 7.5 Hz, 1H, H3-naphthyl), 8.793 (s, 1H, H7-naphthyl), 12.018 (s, 1H, N**CH**N). ^{13}C-NMR (151 MHz, $CDCl_3$): δ = 13.67 (**C**H_3-10-n-butyl), 13.81 (**C**H_3-5-n-butyl), 19.77 (3-**C**H_2-10-n-butyl), 20.34 (3-**C**H_2-5-n-butyl), 21.23 (**C**H_3-(4-methylbenzyl)), 30.00 (2-**C**H_2-5-n-butyl), 31.15 (2-**C**H_2-10-n-butyl), 40.87 (1-**C**H_2-5-n-butyl), 50.99 (1-**C**H_2-10-n-butyl), 51.99 (**C**H_2-(4-methylbenzyl)), 117.21 (C7-naphthyl), 126.70 (C1-naphthyl), 128.44 (H3,5-4-methylbenzyl), 129.76 (C2-naphthyl), 130.31 (H3,5-4-methylbenzyl), 131.54 (C3-naphthyl), 144.61 (N**C**HN), 162.45 (^{4}C4-carbonyl), 163.08 (^{4}C6-carbonyl). $C_{29}H_{32}BrN_3O_2$ (534.49): calcd. C 65.17, H 6.03, N 7.86, found: C 65.32, H 6.08, N 7.89.

General procedure for synthesis of complexes 1 and 3:

Complexes **1** and **3** were prepared according to the literature [45]. A Schlenk tube was charged with a magnetic stir bar, $PdCl_2$ (1.5 eq.), CH_3CN (2 mL, HPLC grade) and *N*,*N*-dimethylbenzylamine (1.5 eq.). The mixture was heated at reflux until a clear, dark orange solution was formed and $PdCl_2$ was dissolved completely (in ~ 25 min). Finely powdered K_2CO_3 (3.5 eq.) was added in one portion, and the mixture was stirred until the solution changed color to bright canary yellow (in ~ 5 min). Relevant imidazolium salt, **NHC.HBr**, (1 eq.) was added in one portion, and the heating at 50°C was continued for another 18 hours. After coiling to room temperature, the reaction mixtures were filtered through a pad of Celite and washed with DCM. After evaporation of solvents, the products were purified by column chromatography (acetone : cyclohexane = 0.5 : 4.5).

General procedure for synthesis of complexes 2 and 4:

Complexes **2** and **4** were prepared according to the literature [46]. A Schlenk tube was charged with a magnetic stir bar, relevant imidazolium salt, **NHC.HBr**, (1 eq.), CH_3CN (2 mL, HPLC grade), *trans*-di(μ-acetato)-bis[o-(di-*o*-tolylphosphino)benzyl]dipalladium(II) (0.75 equiv.) and finely powdered K_2CO_3 (2 equiv.), and the mixture was stirred at 50°C for 18 hours. After coiling to room temperature, the reaction mixtures were filtered through a pad of Celite and washed with DCM. After evaporation of solvents, the products were purified by column chromatography (ethyl acetate : cyclohexane = 0.5 : 4.5).

4.7. **Bromo{2-[(dimethylamino-κ*N*)methyl]phenyl-κ*C*^{1}}[1-[2-(2,6-isopropylphenyl)-1,3-dioxo-2,3-dihydro-1*H*-benzo[*de*]isoquinolin-6-yl]-3-(3-methylbut-2-en-1-yl)-1,3-dihydro-2*H*-imidazol-2-ylidene]palladium** (**1**). Yield

0.18 g (92 %) of white solid with m.p. 120°C (decomposition)**:** ^{1}H-NMR (600 MHz, $CDCl_3$, 223 K): two conformers in 1.1 : 1.0 ratio; Major: δ = 1.072-1.156 (m, 12H, CH**(CH$_3$)$_2$**), 1.788 (s, 3H, a-**(CH$_3$)$_2$**-butenyl), 1.809 (s, 3H, b-**(CH$_3$)$_2$**-butenyl), 2.570 (s, 3H, a-N**(CH$_3$)$_2$**-palladacycle), 2.676-2.755 (m, 2H, C**H**(CH$_3$)$_2$), 2.736 (s, 3H, N**(CH$_3$)$_2$**-palladacycle), 3.706 (d, J = 14.3 Hz, 1H, a-N(CH$_3$)$_2$-**CH$_2$**-palladacycle), 3.773 (d, J = 14.3 Hz, 1H, b-N(CH$_3$)$_2$-**CH$_2$**-palladacycle), 5.181-5.273 (m, 2H, a,b-H1-butenyl), 5.477-5.553 (m, 1H, H2-butenyl), 6.206 (d, J = 7.3 Hz, 1H, H3-palladacycle), 6.632-6.656 (m, 1H, H4-palladacycle), 6.815-6.839 (m, 1H, H5-palladacycle), 6.882 (d, J = 7.0 Hz, 1H, H6-palladacycle), 7.291-7.310 (m, 2H, imidazole), 7.354-7.399 (m, 2H, H3,5-phenyl), 7.524 (t, J = 7.8 Hz, 1H, H4-phenyl), 7.804 (dd, J = 7.0, 8.4 Hz, 1H, H8-naphthyl), 7.994 (d, J = 7.8 Hz, 1H, H5-naphthyl), 8.294 (d, J = 8.4 Hz, 1H, H7-naphthyl), 8.516 (d, J = 7.8 Hz, 1H, H4-naphthyl), 8.639 (d, J = 7.0 Hz, 1H, H9-naphthyl); Minor: δ = 1.072-1.156 (m, 6H, CH**(CH$_3$)$_2$**), 1.189 (d, J=7.0 Hz, 6H, CH**(CH$_3$)$_2$**), 1.799 (s, 3H, b-**(CH$_3$)$_2$**-butenyl), 1.808 (s, 3H, a-**(CH$_3$)$_2$**-butenyl), 2.762 (s, 3H, N**(CH$_3$)$_2$**-palladacycle), 2.766-2.821 (m, 1H, a-C**H**(CH$_3$)$_2$), 2.831-2.902 (m, 1H, b-C**H**(CH$_3$)$_2$), 2.855 (s, 3H, N**(CH$_3$)$_2$**-palladacycle), 3.792 (d, J = 14.3 Hz, 1H, a-N(CH$_3$)$_2$-**CH$_2$**-palladacycle), 3.868 (d, J = 14.3 Hz, 1H, b-N(CH$_3$)$_2$-**CH$_2$**-palladacycle), 5.232 (dd, J = 7.3, 14.5 Hz, 1H, a-H1-butenyl), 5.392 (dd, J = 7.3, 14.5 Hz, 1H, b-H1-butenyl), 5.477-5.553 (m, 1H, H2-butenyl), 6.414 (d, J = 7.3 Hz, 1H, H3-palladacycle), 6.919-6.940 (m, 1H, H4-palladacycle), 7.041-7.080 (m, 2H, H5-palladacycle and H6-palladacycle), 7.291-7.310 (m, 1H, imidazole), 7.354-7.399 (m, 3H, H3,5-phenyl and imidazole), 7.524 (t, J = 7.8 Hz, 1H, H4-phenyl), 7.855 (dd, J = 7.0, 8.4 Hz, 1H, H8-naphthyl), 8.307 (d, J = 8.4 Hz, 1H, H7-naphthyl), 8.705 (d, J = 7.0 Hz, 1H, H9-naphthyl), 8.767 (d, J = 7.8 Hz, 1H, H4-naphthyl), 9.179 (d, J = 7.8 Hz, 1H, H5-naphthyl). ^{13}C NMR (151 MHz, $CDCl_3$, 223 K); Major: δ = 18.62 (a-**(CH$_3$)**-butenyl), 24.28 (CH**(CH$_3$)$_2$**), 24.30 (CH**(CH$_3$)$_2$**), 26.32 (b-**(CH$_3$)**-butenyl), 29.17 (**C**H(CH3)$_2$), 49.86 (C1-butenyl), 50.84 (N**(CH$_3$)$_2$**-palladacycle), 51.00 (N**(CH$_3$)$_2$**-palladacycle), 71.61 (N(CH$_3$)$_2$-**CH$_2$**-palladacycle), 118.32 (C2-butenyl), 121.30 (imidazole), 122.36 (C6-palladacycle), 123.74 (C5-palladacycle), 124.20 (C3-phenyl), 124.25 (C5-phenyl),125.34 (C4-palladacycle), 126.81 (C5-naphthyl), 127.94 (C8-naphthyl), 130.02 (C4-phenyl), 131.00 (C7-naphthyl), 131.16 (C4-naphthyl), 132.42 (C9-naphthyl), 135.50 (C3-palladacycle), 164.24 (^{4}C3-carbonyl), 164.37 (^{4}C1-carbonyl) 174.88 (bs, ^{4}C-carbene); Minor: δ = 18.64 (a-**(CH$_3$)**-butenyl), 24.38 (CH**(CH$_3$)$_2$**), 24.46 (CH**(CH$_3$)$_2$**), 26.35 (b-**(CH$_3$)$_2$**-butenyl), 28.94 (2C, s, C**H**(CH3)$_2$), 50.08 (C1-butenyl), 51.19 (N**(CH$_3$)$_2$**-palladacycle), 51.38 (N**(CH$_3$)$_2$**-palladacycle), 71.74 (N(CH$_3$)$_2$-**CH$_2$**-palladacycle), 118.44 (C2-butenyl), 123.03 (C6-palladacycle), 124.10 (imidazole), 124.36 (C5-palladacycle), 124.61 (C3-phenyl), 124.67 (C5-phenyl), 126.13 (C4-palladacycle), 127.89 (C4-naphthyl), 128.16 (C8-naphthyl), 129.20 (C7-naphthyl), 130.02 (C4-phenyl), 131.71 (C5-naphthyl), 132.93 (C9-naphthyl), 135.70 (C3-palladacycle), 163.70 (^{4}C3-carbonyl), 163.88 (^{4}C1-carbonyl) 174.88 (^{4}bs, ^{4}C-carbene). $C_{41}H_{45}BrN_4O_2Pd$ (810.18): calcd. C 60.63, H 5.58, N 6.90, found: C 60.79, H 5.62, N 6.94.

4.8. **({2-[Bis(2-methylphenyl)phosphanyl-κ*P*]phenyl}methyl-κ*C*)(bromo)[1-[2-(2,6-diisopropylphenyl)-1,3-dioxo-2,3-dihydro-1*H*-benzo[*de*]isoquinolin-6-yl]-3-(3-methylbut-2-en-1-yl)-1,3-dihydro-2*H*-imidazol-2-ylidene]palladium** (**2**). Yield 0.16 g (90 %) of white solid with m.p. 120°C (decomposition)**:** ^{1}H-NMR (600MHz, $CDCl_3$, 223K): four conformers in 1.0 : 0.2 : 0.26 : 0.64 ratio; Major: δ = 1.033 (d, J = 6.5 Hz, 3H, CH**(CH$_3$)$_2$**), 1.162 (d, J = 6.5 Hz, 3H, CH**(CH$_3$)$_2$**), 1.244 (d, J = 6.5 Hz, 3H, CH**(CH$_3$)$_2$**), 1.281 (d, J = 6.5 Hz, 3H, CH**(CH$_3$)$_2$**), 1.651 (s, 3H, **(CH$_3$)$_2$**-butenyl), 1.684 (s, 3H, **(CH$_3$)$_2$**-butenyl), 1.868 (d, J = 13.0 Hz, 1H, a-**CH$_2$**-Pd), 2.302 (s, 3H, **CH$_3$**-o-tol-1), 2.543-2.594 (m, 1H, **CH**(CH$_3$)$_2$), 2.734 (s, 3H, **CH$_3$**-o-tol-2), 2.705-2.777 (m, 1H, **CH**(CH$_3$)$_2$), 2.802 (d, J = 13.0 Hz, 1H, b-**CH$_2$**-Pd), 4.835 (dd, J = 7.4, 14.0 Hz, 1H, a-H1-butenyl), 5.325 (dd, J = 7.4, 14.0 Hz, 1H, b-H1-butenyl), 5.434 (dd, J = 7.4, 7.4 Hz, 1H, H2-butenyl), 6.426-7.46 (m, 14H, 12H of o-tol-1, otol-2 and phosphapalladacycle and 2H of imidazole), 7.383 (d, J = 7.9, 2H, H3,5-phenyl), 7.536 (t, J = 7.9 Hz, 1H, H4-phenyl), 8.016 (dd, J = 7.5, 8.5 Hz, 1H, H8-naphthyl), 8.357 (d, J = 8.5 Hz, 1H, H7-naphthyl), 8.607 (d, J = 7.8 Hz, 1H, H4-naphthyl), 8.702 (d, J = 7.8 Hz, 1H, H5-naphthyl), 8.849 (d, J = 7.5 Hz, 1H, H9-naphthyl). ^{13}C-NMR (251 MHz, $CDCl_3$, 223K); Major: δ = 18.10 (**(C**H$_3$)$_2$-butenyl), 22.97 (d, J=12.30 Hz, **C**H$_3$-o-tol-2), 23.40 (d, J=10.80 Hz, **C**H$_3$-o-tol-1), 23.89 (CH**(C**H$_3$)$_2$), 23.97 (CH**(C**H$_3$)$_2$), 24.04 (CH**(C**H$_3$)$_2$), 24.06 (CH**(C**H$_3$)$_2$), 24.29 (**C**H$_2$-Pd), 25.91 (**(C**H$_3$)$_2$-butenyl), 28.84 (**C**H(CH$_3$)$_2$), 28.91 (**C**H(CH$_3$)$_2$), 49.09 (C1-butenyl), 118.69 (C2-butenyl), 124.2 (C3,5-phenyls), 128.17 (C8-naphthyl), 129.19 (C7-naphthyl), 129.22 (C5-naphthyl), 129.76 (C4-phenyl), 131.48 (C4-naphthyl), 132.34 (C9-naphthyl), 163.12 (^{4}C3-carbonyl), 163.97 (^{4}C1-carbonyl), 181.79 (d, $^{2}J_{C\text{-}P\text{-}trans}$ = 144.5 Hz, ^{4}C-carbene). ^{31}P{^{1}H}-NMR (243 MHz, $CDCl_3$, 223K); four conformers in 1.0 : 0.2 : 0.26 : 0.64 ratio; δ = 27.45, 28.64, 31.31, 31.58 ppm. $C_{53}H_{53}BrN_3O_2PPd$ (979.21): calcd. C 64.87, H 5.44, N, 4.28, found: C 65.02, H 5.52, N 4.31.

4.9. **[5,10-Dibutyl-8-(4-methylbenzyl)-4,6-dioxo-5,6,8,10-tetrahydrobenzo[*de*]imidazo[4,5-*g*]isoquinolin-9(4*H*)-ylidene](bromo){2-[(dimethylamino-κ*N*)methyl]phenyl-κ*C*^{1}}palladium (3)**. Yield 0.14 g (80 %) of pale yellow solid with m.p. 120°C (decomposition)**:** ^{1}H NMR (600 MHz, $CDCl_3$): δ = 0.967 (t, J = 7.4 Hz, 3H, **CH$_3$**-10-n-butyl), 1.075 (t, J = 7.4 Hz, 3H, **CH$_3$**-5-n-butyl), 1.402-1.464 (m, 2H, 3-**CH$_2$**-10-n-butyl), 1.622-1.679 (m, 2H, 2-**CH$_2$**-5-n-

butyl), 1.679-1.722 (m, 2H, 3-**CH$_2$**-10-n-butyl), 2.017-2.091 (m, 1H, a-2-**CH$_2$**-10-n-butyl), 2.254 (s, 3H, **CH$_3$**-(4-methylbenzyl)), 2.331-2.406 (m, 1H, b-2-**CH$_2$**-10-n-butyl), 2.942 (s, 3H, a-N(**CH$_3$**)$_2$-palladacycle) 2.950 (s, 3H, b-N(**CH$_3$**)$_2$-palladacycle), 3.914 (d, J = 14.1 Hz, 1H, a-N(CH$_3$)$_2$-**CH$_2$**-palladacycle), 4.061 (d, J = 14.1 Hz, 1H, b-N(CH$_3$)$_2$-**CH$_2$**-palladacycle), 4.143-4.167 (m, 2H, 1-**CH$_2$**-5-n-butyl), 5.297-5.342 (m, 1H, a-1-**CH$_2$**-10-n-butyl), 5.4029-5.453 (m, 1H, a-1-**CH$_2$**-10-n-butyl), 5.958 (d, J = 15.4 Hz, 1H, a-**CH$_2$**-(4-methylbenzyl)), 5.972 (dd, J = 1.0, 7.5 Hz, 1H, H6-palladacycle), 6.215 (d, J = 15.4 Hz, 1H, b-**CH$_2$**-(4-methylbenzyl)), 6.641 (ddd, J = 1.0, 7.4, 7.5 Hz, 1H, H5-palladacycle), 6.958 (ddd, J = 0.8, 7.4, 7.5 Hz, 1H, H4-palladacycle), 7.044 (dd, J = 0.8, 7.4 Hz, 1H, H3-palladacycle), 7.075 (d, J = 8.0 Hz, 2H, H2,6-4-methylbenzyl), 7.447 (d, J = 8.0 Hz, 2H, H3,5-4-methylbenzyl), 7.937 (dd, J = 7.4, 8.3 Hz, 1H, H2-naphthyl), 8.559 (s, 1H, H7-naphthyl), 8.641 (dd, J = 1.0, 8.3 Hz, 1H, H1-naphthyl), 8.678 (dd, J = 1.0, 7.4 Hz, 1H, H3-naphthyl).^{13}C NMR (151 MHz, $CDCl_3$): δ = 13.73 (**CH$_3$**-10-n-butyl), 13.86 (**CH$_3$**-5-n-butyl), 20.16 (2-**CH$_2$**-5-n-butyl), 20.41 (3-**CH$_2$**-5-n-butyl), 21.16 (**CH$_3$**-(4-methylbenzyl)), 30.13 (3-**CH$_2$**-10-n-butyl), 30.74 (2-**CH$_2$**-10-n-butyl), 40.60 (1-**CH$_2$**-5-n-butyl), 50.88 (a-N(**CH$_3$**)$_2$-palladacycle), 51.41 (b-N(**CH$_3$**)$_2$-palladacycle), 52.04 (1-**CH$_2$**-10-n-butyl), 54.13 (**CH$_2$**-(4-methylbenzyl)), 72.28 (N(CH$_3$)$_2$-**CH$_2$**-palladacycle), 116.82 (C7-naphthyl), 122.60 (C3-palladacycle), 124.31 (C4-palladacycle), 125.74 (C5-palladacycle), 126.93 (C1-naphthyl), 127.92 (C3-naphthyl), 128.18 (C3,5-4-methylbenzyl), 129.67 (C3,5-4-methylbenzyl), 129.98 (C3-naphthyl), 135.49 (C6-palladacycle), 163.54 (^{4}C6-carbonyl), 163.99 (^{4}C4-carbonyl), 188.99 (^{4}C, Pd-carbene). $C_{38}H_{43}BrN_4O_2Pd$ (772.16): calcd. C 58.96, H 5.60, N 7.24, found: C 59.04, H 5.66, N 7.27.

4.10. **({2-[Bis(2-methylphenyl)phosphanyl-κ*P*]phenyl}methyl-κ*C*)(bromo)[5,10-dibutyl-8-(4-methylbenzyl)-4,6-dioxo-5,6,8,10-tetrahydrobenzo[*de*]imidazo[4,5-*g*]isoquinolin-9(4*H*)-ylidene]palladium (4)**. Yield 70 mg (83 %) of pale yellow solid with m.p. 120°C (decomposition)**:** ^{1}H-NMR (600 MHz, $CDCl_3$, 233 K); two conformers in 1.59 : 1.0 ratio; Major: δ = 0.959 (t, 3H, **CH$_3$**-5-n-butyl), 0.972 (t, 3H, **CH$_3$**-10-n-butyl), 1.401-1.472 (m, 2H, 3-**CH$_2$**-5-n-butyl), 1.482-1.574 (m, 2H, 3-**CH$_2$**-10-n-butyl), 1.648-1.715 (m, 2H, 2-**CH$_2$**-5-n-butyl), 1.961-2.055 (m, 1H, a-2-**CH$_2$**-10-n-butyl), 2.138 (s, 3H, **CH$_3$**-(4-methylbenzyl), 2.272-2.365 (m, 1H, b-2-**CH$_2$**-10-n-butyl), 2.363 (d, J = 13.0 Hz, 1H, a-**CH$_2$**-Pd), 2.645 (d, J = 13.0 Hz, 1H, b-**CH$_2$**-Pd), 2.918 (s, 3H, **CH$_3$**-o-tol-2), 2.924 (s, 3H, **CH$_3$**-o-tol-1), 4.141-4.1715 (m, 2H, 1-**CH$_2$**-5-n-butyl), 5.112-5.181 (m, 1H, a-1-**CH$_2$**-10-n-butyl), 5.284-5.337 (m, 1H, b-1-**CH$_2$**-10-n-butyl), 5.677 (d, J = 15.0 Hz, 1H, a-**CH$_2$**-(4-methylbenzyl)), 5.993 (d, J = 15.0 Hz, 1H, b-**CH$_2$**-(4-methylbenzyl)), 6.697 (d, J = 8.1 Hz, 2H, H3,5-4-methylbenzyl), 6.732-6.762 (m, 1H, Ar-phosphapalladacycle), 6.884-7.516 [(13H: 6.881-6.907 (m, 1H, o-tol-1), 6.986-6.994 (m, 1H, o-tol-2), 7.011-7.016 (m, 1H, Ar-phosphapalladacycle), 7.043-7.064 (m, 1H, Ar-phosphapalladacycle), 7.183-7.205 (m, 1H, o-tol-2), 7.188-7.214 (m, 1H, Ar-phosphapalladacycle), 7.215 (d, J = 8.1 Hz, 2H, H2,6-4-methylbenzyl), 7.224-7.237 (m, 1H, o-tol-1), 7.241-7.264 (m, 1H, o-tol-2), 7.334-7.381 (m, 1H, o-tol-2), 7.481-7.517 (m, 2H, o-tol-1)], 7.975 (dd, J = 8.5, 7.4 Hz, 1H, H2-naphthyl), 8.593 (dd, J = 0.9, 8.5 Hz, 1H, H1-naphthyl), 8.696 (dd, J = 0.9, 7.4 Hz, 1H, H3-naphthyl), 8.703(s, 1H, H7-naphthyl). Minor: δ = 0.82 (t, J = 7.3 Hz, 3H, **CH$_3$**-10-n-butyl), 0.9511 (t, J = 7.3, 3H, **CH$_3$**-5-n-butyl), 1.401-1.472 (m, 4H, 3-**CH$_2$**-5-n-butyl and 3-**CH$_2$**-10-n-butyl), 1.648-1.715 (m, 2H, 2-**CH$_2$**-5-n-butyl), 1.789-1.867 (m, 1H, a-2-**CH$_2$**-10-n-butyl), 2.158-2.227 (m, 1H, b-2-**CH$_2$**-10-n-butyl), 2.291 (s, 3H, **CH$_3$**-(4-methylbenzyl)), 2.583 (d, J = 13.0 Hz, 1H, a-**CH$_2$**-Pd), 2.723 (s, 3H, **CH$_3$**-o-tol-2), 2.796 (s, 3H, **CH$_3$**-o-tol-1), 3.218 (d, J = 13.0 Hz, 1H, b-**CH$_2$**-Pd), 4.141-4.1715 (m, 2H, 1-**CH$_2$**-5-n-butyl), 4.929-4.981 (m, 1H, a-1-**CH$_2$**-10-n-butyl), 5.112-5.181 (m, 1H, b-1-**CH$_2$**-10-n-butyl), 5.872 (d, J = 15.0 Hz, 1H, a-**CH$_2$**-(4-methylbenzyl)), 6.324 (d, J = 15.0 Hz, 1H, b-**CH$_2$**-(4-methylbenzyl)), 6.75-6.78 (m, 1H, Ar-phosphapalladacycle), 6.884-7.516 [(16H: 6.935-6.951 (m, 1H, o-tol-1), 6.946-6.988 (m, 1H, Ar-phosphapalladacycle), 6.997-7.012 (m, 1H, o-tol-2), 7.022-7.034 (m, 1H, Ar-phosphapalladacycle), 7.064 (d, J = 8.1 Hz, 2H, H3,5-4-methylbenzyl), 7.127-7.172 (m, 2H, o-tol-1), 7.184-7.214 (m, 1H, Ar-phosphapalladacycle), 7.187-7.225 (m, 1H, o-tol-2), 7.266-7.278 (m, 1H, o-tol-2), 7.341-7.379 (m, 1H, o-tol-2), 7.428-7.433 (m, 2H, o-tol-1), 7.478 (d, J = 8.1 Hz, 2H, H2,6-4-methylbenzyl)], 7.931 (dd, J = 8.5, 7.4 Hz, 1H, H2-naphthyl), 8.528 (dd, J = 0.9, 8.5 Hz, 1H, H1-naphthyl), 8.662 (dd, J = 0.9, 7.4 Hz, 1H, H3-naphthyl), 8.684 (s, 1H, H7-naphthyl). ^{13}C-NMR (151MHz, $CDCl_3$, 233 K); Major: δ = 14.27 (**CH$_3$**-10-n-butyl-major), 14.30 (**CH$_3$**-5-n-butyl), 20.54 (C3-**CH$_2$**-10-n-butyl), 20.64 (C3-**CH$_2$**-5-n-butyl), 21.46 (**CH$_3$**-(4-methylbenzyl)), 22.64 (**CH$_2$**-Pd-major), 23.12 (d, $^3J_{C\text{-}P}$ = 11.7 Hz, **CH$_3$**-o-tol-2), 23.81 (d, $^3J_{C\text{-}P}$ = 9.0 Hz, **CH$_3$**-o-tol-1), 30.21 (C2-**CH$_2$**-5-n-butyl), 31.82 (C2-**CH$_2$**-10-n-butyl), 40.87 (C1-**CH$_2$**-5-n-butyl), 52.10 (C1-**CH$_2$**-10-n-butyl), 52.34 (**CH$_2$**-(4-methylbenzyl)), 116.48 (C7-naphthyl), 125.80 (Ar-phosphapalladacycle), 126.20 (d, $^2J_{C\text{-}P}$ = 4.0 Hz, o-tol-2), 126.74 (d, $^3J_{C\text{-}P}$ =18.0 Hz, Ar-phosphapalladacycle), 127.18 (C1-naphthyl), 128.36 (C2-naphthyl), 128.37 (C2,6-(4-methylbenzyl)), 129.48 (C3,5-(4-methylbenzyl)), 130.25 (C3-naphthyl), 130.50 (o-tol-1), 130.80 (o-tol-2), 130.95 (Ar-phosphapalladacycle), 131.56 (d, $J_{C\text{-}P}$ = 7.7 Hz, o-tol-1), 131.79 (d, $J_{C\text{-}P}$ = 8.4 Hz, o-tol-2), 132.43 (Ar-phosphapalladacycle), 133.00 (o-tol-1), 133.14 (o-tol-2),), 134.08 (d, $^1J_{C\text{-}P}$ = 49.0 Hz, ipso-P-Ar-phosphapalladacycle-major), 162.68 (^{4}C6-carbonyl), 163.02 (^{4}C6-carbonyl), 195.81 (d, $^2J_{C\text{-}}$

$_{P\text{-}trans}$ = 142.0 Hz, ^{4}C-carbene). Minor: δ = 13.63 (**CH$_3$**-10-n-butyl), 14.30 (**CH$_3$**-5-n-butyl), 20.05 (C3-**CH$_2$**-10-n-butyl), 20.64 (C3-**CH$_2$**-5-n-butyl), 21.55 (**CH$_3$**-(4-methylbenzyl)), 22.66 (**CH$_2$**-Pd), 23.22 (d, $^{3}J_{C\text{-}P}$ = 11.7 Hz, **CH$_3$**-o-tol-2), 23.97 (d, $^{3}J_{C\text{-}P}$ = 9.0 Hz, **CH$_3$**-o-tol-1), 30.19 (C2-**CH$_2$**-5-n-butyl), 31.53 (C2-**CH$_2$**-10-n-butyl), 40.89 (C1-**CH$_2$**-5-n-butyl), 51.45 (C1-**CH$_2$**-10-n-butyl), 52.84 (**CH$_2$**-(4-methylbenzyl)), 116.83 (C7-naphthyl), 125.80 (Ar-phosphapalladacycle), 125.84 (o-tol-1), 126.15 (d, $^{2}J_{C\text{-}P}$ = 4.0 Hz, o-tol-2), 127.17 (C1-naphthyl), 127.19 (d, $^{3}J_{C\text{-}P}$ = 18.0 Hz, Ar-phosphapalladacycle), 128.13 (C2,6-(4-methylbenzyl)), 129.88 (C3,5-(4-methylbenzyl)), 130.23 (C3-naphthyl), 130.42 (o-tol-1), 130.80 (o-tol-2), 130.86 (Ar-phosphapalladacycle), 131.31 (d, $^{2}J_{C\text{-}P}$ = 7.7 Hz, o-tol-1), 131.69 (d, $^{2}J_{C\text{-}P}$ = 8.4 Hz, o-tol-2), 132.14 (Ar-phosphapalladacycle), 132.98 (d, $^{2}J_{C\text{-}P}$ = 6.0 Hz, o-tol-1), 133.14 (o-tol-2), 133.87 (d, $^{1}J_{C\text{-}P}$ = 49.0 Hz, ipso-P-Ar-phosphapalladacycle), 162.59 (^{4}C6-carbonyl), 163.02 (^{4}C6-carbonyl), 195.37 (d, $^{2}J_{C\text{-}P\text{-}trans}$ = 142.0 Hz, ^{4}C-carbene). ^{31}P{^{1}H}-NMR (243 MHz, $CDCl_3$, 233 K); two conformers in 1.59 : 1.0 ratio; δ = 28.65 (minor), 29.59 (major) ppm. $C_{50}H_{51}BrN_3O_2PPd$ (941.19): calcd. C 63.67, H 5.45, N 4.45, found: C 63.82, H 5.53, N 4.46.

Appendix A. Supplementary data

Supplementary data related to this article (copies of the ^{1}H, ^{13}C and ^{31}P NMR spectra of the new complexes, details of dynamic NMR studies and DFT calculations) are provided.

Acknowledgement The financial support by the Bulgarian Science Fund (Projects UNA-17/2005, RNF01/0110 and DRNF-02/13)**,** the Sofia University Research Fund (143/05.2010) and COST action CM0802 ‘‘PhoSciNet” is gratefully acknowledged.

References:

[1] W.A. Herrmann, C. Köcher, Angew. Chem. Int. Ed. Engl., 36 (1997) 2162-2187.
[2] D. Bourissou, O. Guerret, F.P. Gabbaï, G. Bertrand, Stable Carbenes, Chemical Reviews, 100 (2000) 39-91.
[3] F.E. Hahn, M.C. Jahnke, Heterocyclic carbenes: Synthesis and coordination chemistry, Angewandte Chemie - International Edition, 47 (2008) 3122-3172.
[4] J.C.Y. Lin, R.T.W. Huang, C.S. Lee, A. Bhattacharyya, W.S. Hwang, I.J.B. Lin, Coinage metal-N-heterocyclic carbene complexes, Chemical Reviews, 109 (2009) 3561-3598.
[5] P.L. Arnold, I.J. Casely, F-block N-heterocyclic carbene complexes, Chemical Reviews, 109 (2009) 3599-3611.
[6] O. Schuster, L. Yang, H.G. Raubenheimer, M. Albrecht, Beyond conventional N-heterocyclic carbenes: Abnormal, remote, and other classes of NHC ligands with reduced heteroatom stabilization, Chemical Reviews, 109 (2009) 3445-3478.
[7] W.A. Herrmann, N-heterocyclic carbenes: A new concept in organometallic catalysis, Angewandte Chemie - International Edition, 41 (2002) 1290-1309.
[8] S. Díez-González, N. Marion, S.P. Nolan, N-heterocyclic carbenes in late transition metal catalysis, Chemical Reviews, 109 (2009) 3612-3676.
[9] G.C. Fortman, S.P. Nolan, N-Heterocyclic carbene (NHC) ligands and palladium in homogeneous cross-coupling catalysis: A perfect union, Chemical Society Reviews, 40 (2011) 5151-5169.
[10] C. Valente, S. Çalimsiz, K.H. Hoi, D. Mallik, M. Sayah, M.G. Organ, The development of bulky palladium NHC complexes for the most-challenging cross-coupling reactions, Angewandte Chemie - International Edition, 51 (2012) 3314-3332.
[11] H. Seo, B.Y. Kim, J.H. Lee, H.J. Park, S.U. Son, Y.K. Chung, Synthesis of chiral ferrocenyl imidazolium salts and their rhodium(I) and iridium(I) complexes, Organometallics, 22 (2003) 4783-4791.
[12] H.V. Huynh, L.R. Wong, P.S. Ng, Anagostic interactions and catalytic activities of sterically bulky benzannulated N-heterocyclic carbene complexes of nickel(II), Organometallics, 27 (2008) 2231-2237.
[13] D. Yuan, H. Tang, L. Xiao, H.V. Huynh, CSC-pincer versus pseudo-pincer complexes of palladium(ii): A comparative study on complexation and catalytic activities of NHC complexes, Dalton Transactions, 40 (2011) 8788-8795.
[14] L. Busetto, M.C. Cassani, C. Femoni, M. Mancinelli, A. Mazzanti, R. Mazzoni, G. Solinas, N-heterocyclic carbene-amide rhodium(I) complexes: Structures, dynamics, and catalysis, Organometallics, 30 (2011) 5258-5272.
[15] O. Kühl, The chemistry of functionalised N-heterocyclic carbenes, Chemical Society Reviews, 36 (2007) 592-607.
[16] A. John, P. Ghosh, Fascinating frontiers of N/O-functionalized N-heterocyclic carbene chemistry: From chemical catalysis to biomedical applications, Dalton Transactions, 39 (2010) 7183-7206.

[17] C. Fliedel, P. Braunstein, Recent advances in S-functionalized N-heterocyclic carbene ligands: From the synthesis of azolium salts and metal complexes to applications, Journal of Organometallic Chemistry, 751 (2014) 286-300.
[18] A.T. Normand, K.J. Cavell, Donor-functionalised N-heterocyclic carbene complexes of group 9 and 10 metals in catalysis: Trends and directions, European Journal of Inorganic Chemistry, (2008) 2781-2800.
[19] M. Bierenstiel, E.D. Cross, Sulfur-functionalized N-heterocyclic carbenes and their transition metal complexes, Coordination Chemistry Reviews, 255 (2011) 574-590.
[20] H.V. Huynh, C.H. Yeo, G.K. Tan, Hemilabile behavior of a thioether-functionalized N-heterocyclic carbene ligand, Chemical Communications, (2006) 3833-3835.
[21] H.V. Huynh, C.H. Yeo, Y.X. Chew, Syntheses, structures, and catalytic activities of hemilabile thioether-functionalized NHC complexes, Organometallics, 29 (2010) 1479-1486.
[22] M.V. Jiménez, J. Fernández-Tornos, J.J. Pérez-Torrente, F.J. Modrego, S. Winterle, C. Cunchillos, F.J. Lahoz, L.A. Oro, Iridium(I) complexes with hemilabile N-heterocyclic carbenes: Efficient and versatile transfer hydrogenation catalysts, Organometallics, 30 (2011) 5493-5508.
[23] J. Lemke, N. Metzler-Nolte, The synthesis of ruthenium and rhodium complexes with functionalized N-heterocyclic carbenes and their use in solid phase peptide synthesis, European Journal of Inorganic Chemistry, (2008) 3359-3366.
[24] E. Chardon, G.L. Puleo, G. Dahm, G. Guichard, S. Bellemin-Laponnaz, Direct functionalisation of group 10 N-heterocyclic carbene complexes for diversity enhancement, Chemical Communications, 47 (2011) 5864-5866.
[25] S. Roland, C. Jolivalt, T. Cresteil, L. Eloy, P. Bouhours, A. Hequet, V. Mansuy, C. Vanucci, J.M. Paris, Investigation of a series of silver-N-Heterocyclic carbenes as antibacterial agents: Activity, synergistic effects, and cytotoxicity, Chemistry - A European Journal, 17 (2011) 1442-1446.
[26] T.H.T. Hsu, J.J. Naidu, B.J. Yang, M.Y. Jang, I.J.B. Lin, Self-assembly of silver(I) and gold(I) N-heterocyclic carbene complexes in solid state, mesophase, and solution, Inorganic Chemistry, 51 (2012) 98-108.
[27] A. Azua, S. Sanz, E. Peris, Water-soluble IrIII N-heterocyclic carbene based catalysts for the reduction of CO2 to formate by transfer hydrogenation and the deuteration of aryl amines in water, Chemistry - A European Journal, 17 (2011) 3963-3967.
[28] G. Li, H. Yang, W. Li, G. Zhang, Rationally designed palladium complexes on a bulky N-heterocyclic carbene-functionalized organosilica: An efficient solid catalyst for the Suzuki-Miyaura coupling of challenging aryl chlorides, Green Chemistry, 13 (2011) 2939-2947.
[29] H.D. Velazquez, F. Verpoort, N-heterocyclic carbene transition metal complexes for catalysis in aqueous media, Chemical Society Reviews, 41 (2012) 7032-7060.
[30] L.A. Schaper, S.J. Hock, W.A. Herrmann, F.E. Kühn, Synthesis and application of water-soluble NHC transition-metal complexes, Angewandte Chemie - International Edition, 52 (2013) 270-289.
[31] E.A.B. Kantchev, C.J. O'Brien, M.G. Organ, Palladium complexes of N-heterocyclic carbenes as catalysts for cross-coupling reactions - A synthetic chemist's perspective, Angewandte Chemie - International Edition, 46 (2007) 2768-2813.
[32] J.P. Sauvage, J.P. Collin, J.C. Chambron, S. Guillerez, C. Coudret, V. Balzani, F. Barigelletti, L. De Cola, L. Flamigni, Ruthenium(II) and osmium(II) bis(terpyridine) complexes in covalently-linked multicomponent systems: Synthesis, electrochemical behavior, absorption spectra, and photochemical and photophysical properties, Chemical Reviews, 94 (1994) 993-1019.
[33] L. Cavallo, A. Correa, C. Costabile, H. Jacobsen, Steric and electronic effects in the bonding of N-heterocyclic ligands to transition metals, Journal of Organometallic Chemistry, 690 (2005) 5407-5413.
[34] F.E. Hahn, Heterocyclic Carbenes, Angewandte Chemie - International Edition, 45 (2006) 1348-1352.
[35] R. Dorta, N.M. Scott, C. Costabile, L. Cavallo, C.D. Hoff, S.P. Nolan, Steric and electronic properties of N-heterocyclic carbenes (NHC): A detailed study on their interaction with Ni(CO)₄, Journal of the American Chemical Society, 127 (2005) 2485-2495.
[36] A.R. Chianese, X. Li, M.C. Janzen, J.W. Faller, R.H. Crabtree, Rhodium and iridium complexes of N-heterocyclic carbenes via transmetalation: Structure and dynamics, Organometallics, 22 (2003) 1663-1667.
[37] W.A. Herrmann, J. Schütz, G.D. Frey, E. Herdtweck, N-heterocyclic carbenes: Synthesis, structures, and electronic ligand properties, Organometallics, 25 (2006) 2437-2448.
[38] C.J. O'Brien, E.A.B. Kantchev, G.A. Chass, N. Hadei, A.C. Hopkinson, M.G. Organ, D.H. Setiadi, T.H. Tang, D.C. Fang, Towards the rational design of palladium-N-heterocyclic carbene catalysts by a combined experimental and computational approach, Tetrahedron, 61 (2005) 9723-9735.
[39] S. Stoyanov, P. Petrov, M. Stoyanova, M. Dangalov, B. Shivachev, R. Nikolova, I. Petkov, 4-Amino-3-nitro naphthalimides-structures and spectral properties, Journal of Photochemistry and Photobiology A: Chemistry, 250 (2012) 92-98.

[40] P.A. Panchenko, O.A. Fedorova, Y.V. Fedorov, Fluorescent and colorimetric chemosensors for cations based on 1,8-naphthalimide derivatives: Design principles and optical signalling mechanisms, Russian Chemical Reviews, 83 (2014) 155-182.
[41] I. Philipova, G. Stavrakov, N. Vassilev, R. Nikolova, B. Shivachev, V. Dimitrov, Cytisine as a scaffold for ortho-diphenylphosphinobenzenecarboxamide ligands for Pd-catalyzed asymmetric allylic alkylation, Journal of Organometallic Chemistry, 778 (2015) 10-20.
[42] M. Ehn, N.G. Vassilev, L.F. Pašteka, M. Dangalov, M. Putala, Atropisomerism of 2,2′-Diaryl-1,1′-binaphthalenes Containing Three Stereo-genic Axes: Experimental and Computational Study, European Journal of Organic Chemistry, 2015 (2015) 7935-7942.
[43] A.M. Kadhim, A.T. Peters, New Intermediates and Dyes for Synthetic–polymer Fibres 4–(4–Methoxyanilino)–3–nitro–l, 8–naphthalimides, Journal of the Society of Dyers and Colourists, 90 (1974) 153-157.
[44] L. Zhu, L. Cheng, Y. Zhang, R. Xie, J. You, Highly Efficient Copper-Catalyzed N-Arylation of Nitrogen-Containing Heterocycles with Aryl and Heteroaryl Halides, The Journal of Organic Chemistry, 72 (2007) 2737-2743.
[45] E.A.B. Kantchev, J.Y. Ying, Practical One-Pot, Three-Component Synthesis of N-Heterocyclic Carbene (NHC) Ligated Palladacycles Derived from N,N-Dimethylbenzylamine, Organometallics, 28 (2009) 289-299.
[46] G.D. Frey, J. Schütz, W.A. Herrmann, A straight forward in situ preparation of NHC-substituted phosphapalladacycles, Journal of Organometallic Chemistry, 691 (2006) 2403-2408.
[47] E.M. Viviente, P.S. Pregosin, D. Schott, NMR Spectroscopy and Homogeneous Catalysis, in: Mechanisms in Homogeneous Catalysis, Wiley-VCH Verlag GmbH & Co. KGaA, 2005, pp. 1-80.
[48] D. Drago, P.S. Pregosin, Allyl, olefin, aryl and alkyl organometallic palladium complexes of 1,2-bis[(2R,5R)-2,5-dimethylphospholanyl]benzene, Journal of the Chemical Society, Dalton Transactions, (2000) 3191-3196.
[49] W.A. Herrmann, V.P.W. Böhm, C.P. Reisinger, Application of palladacycles in Heck type reactions, Journal of Organometallic Chemistry, 576 (1999) 23-41.
[50] G.S. Kottas, L.I. Clarke, D. Horinek, J. Michl, Artificial molecular rotors, Chemical Reviews, 105 (2005) 1281-1376.
[51] K. Mislow, Stereochemical consequences of correlated rotation in molecular propellers, Accounts of Chemical Research, 9 (1976) 26-33.
[52] E.E. Wille, D.S. Stephenson, P. Capriel, G. Binsch, Iterative analysis of exchange-broadened NMR band shapes. The mechanism of correlated rotations in triaryl derivatives of phosphorus and arsenic, Journal of the American Chemical Society, 104 (1982) 405-415.
[53] J.A.J. Jarvis, R.H.B. Mais, P.G. Owston, D.T. Thompson, J. Chem. Soc. A, (1968) 622.
[54] J.A.J. Jarvis, R.H.B. Mais, P.G. Owston, D.T. Thompson, A.M. Woop, J. Chem. Soc. A, (1967) 1744.
[55] A.K. Colter, I.I. Schuster, R.J. Kurland, Fluorine magnetic resonance studies of conformational equilibria in triphenylcarbonium ions [1], Journal of the American Chemical Society, 87 (1965) 2278-2279.
[56] R.J. Kurland, I.I. Schuster, A.K. Colter, Fluorine magnetic resonance studies of conformational interconversion rates in triphenylcarbonium ions [2], Journal of the American Chemical Society, 87 (1965) 2279-2281.
[57] A.C. Tsipis, DFT flavor of coordination chemistry, Coordination Chemistry Reviews, 272 (2014) 1-29.
[58] H.M. Lee, J.Y. Zeng, C.H. Hu, M.T. Lee, A new tridentate pincer phosphine/N-heterocyclic carbene ligand: Palladium complexes, their structures, and catalytic activities, Inorganic Chemistry, 43 (2004) 6822-6829.
[59] H.V. Huynh, J. Wu, Rotamers of palladium complexes bearing IR active N-heterocyclic carbene ligands: Synthesis, structural characterization and catalytic activities, Journal of Organometallic Chemistry, 694 (2009) 323-331.
[60] M.M. Gallagher, A.D. Rooney, J.J. Rooney, Variable temperature 1H NMR studies on Grubbs catalysts, Journal of Organometallic Chemistry, 693 (2008) 1252-1260.
[61] R.K. Mackenzie, D.D. MacNicol, J. Chem. Soc., Chem. Commun., (1970).
[62] F.M. Rivas, A.J. Giessert, S.T. Diver, Aromatic Amination/Imination Approach to Chiral Benzimidazoles, The Journal of Organic Chemistry, 67 (2002) 1708-1711.
[63] W.A. Herrmann, V.P.W. Böhm, C.P. Reisinger, Introduction to Homogeneous Catalysis: Carbon-Carbon Bond Formation Catalyzed by a Defined Palladium Complex, Journal of Chemical Education, 77 (2000) 92-95.
[64] A. Lidén, J. Sandström, Barriers to topomerization* in iminodithiocarbonates. A hammett correlation and complete lineshape study, Tetrahedron, 27 (1971) 2893-2901.
[65] EXSYcalc v. 1.0, MestreLab Research S. L., http://mestrelab.com.
[66] G. Binsch, in: L.M. Jackman, F.A. Cotton (Eds.) Dynamic NMR spectroscopy, Academic Press, New York, 1975, pp. 45-82.

[67] J. Heinzer, J.F.M. Oth, Iterative Least-Squares Lineshape Fitting of H-1-Decoupled C-13-Dnmr Spectra, Helvetica Chimica Acta, 64 (1981) 258-278.
[68] P. Hohenberg, W. Kohn, Inhomogeneous electron gas, Physical Review, 136 (1964) B864-B871.
[69] W. Kohn, L.J. Sham, Quantum density oscillations in an inhomogeneous electron gas, Physical Review, 137 (1965) A1697-A1705.
[70] R.G. Parr, W. Yang, Density Functional Theory of Atoms and Molecules, Oxford Univ Press, Oxford, 1989.
[71] M.J.T. Frisch, G. W.; Schlegel, H. B.; Scuseria, G. E.; Robb, M. A.; Cheeseman, J. R.; Scalmani, G.; Barone, V.; Mennucci, B.; Petersson, G. A.; Nakatsuji, H.; Caricato, M.; Li, X.; Hratchian, H. P.; Izmaylov, A. F.; Bloino, J.; Zheng, G.; Sonnenberg, J. L.; Hada, M.; Ehara, M.; Toyota, K.; Fukuda, R.; Hasegawa, J.; Ishida, M.; Nakajima, T.; Honda, Y.; Kitao, O.; Nakai, H.; Vreven, T.; Montgomery, Jr., J. A.; Peralta, J. E.; Ogliaro, F.; Bearpark, M.; Heyd, J. J.; Brothers, E.; Kudin, K. N.; Staroverov, V. N.; Kobayashi, R.; Normand, J.; Raghavachari, K.; Rendell, A.; Burant, J. C.; Iyengar, S. S.; Tomasi, J.; Cossi, M.; Rega, N.; Millam, N. J.; Klene, M.; Knox, J. E.; Cross, J. B.; Bakken, V.; Adamo, C.; Jaramillo, J.; Gomperts, R.; Stratmann, R. E.; Yazyev, O.; Austin, A. J.; Cammi, R.; Pomelli, C.; Ochterski, J. W.; Martin, R. L.; Morokuma, K.; Zakrzewski, V. G.; Voth, G. A.; Salvador, P.; Dannenberg, J. J.; Dapprich, S.; Daniels, A. D.; Farkas, Ö.; Foresman, J. B.; Ortiz, J. V.; Cioslowski, J.; Fox, D. J., in, Gaussian, Inc., Wallingford CT, 2009.
[72] A.D. Becke, Density-functional thermochemistry. III. The role of exact exchange, The Journal of Chemical Physics, 98 (1993) 5648-5652.
[73] C. Lee, W. Yang, R.G. Parr, Development of the Colle-Salvetti correlation-energy formula into a functional of the electron density, Physical Review B, 37 (1988) 785-789.
[74] W.R. Wadt, P.J. Hay, Ab initio effective core potentials for molecular calculations. Potentials for main group elements Na to Bi, The Journal of Chemical Physics, 82 (1985) 284-298.
[75] A.V. Marenich, C.J. Cramer, D.G. Truhlar, Universal solvation model based on solute electron density and on a continuum model of the solvent defined by the bulk dielectric constant and atomic surface tensions, Journal of Physical Chemistry B, 113 (2009) 6378-6396.

- Four catalytically relevant Pd(II) NHC complexes involving bidentate N- and P-donor ligands were synthesized and characterized
- The structures and conformations of the complexes were elucidated on the basis of combination of dynamic NMR and DFT studies
- The results from dynamic NMR and DFT studies confirmed hindered rotation around C-N bond in 1,3-disubstituted imidazole complexes
- The fluxional behavior of P-donor ligands includes exchange between left-handed and right-handed phosphine propellers
- The palladium complexes **3** and **4** were evaluated as catalysts in Suzuki–Miyaura Reaction and exhibited excellent catalytic activity.